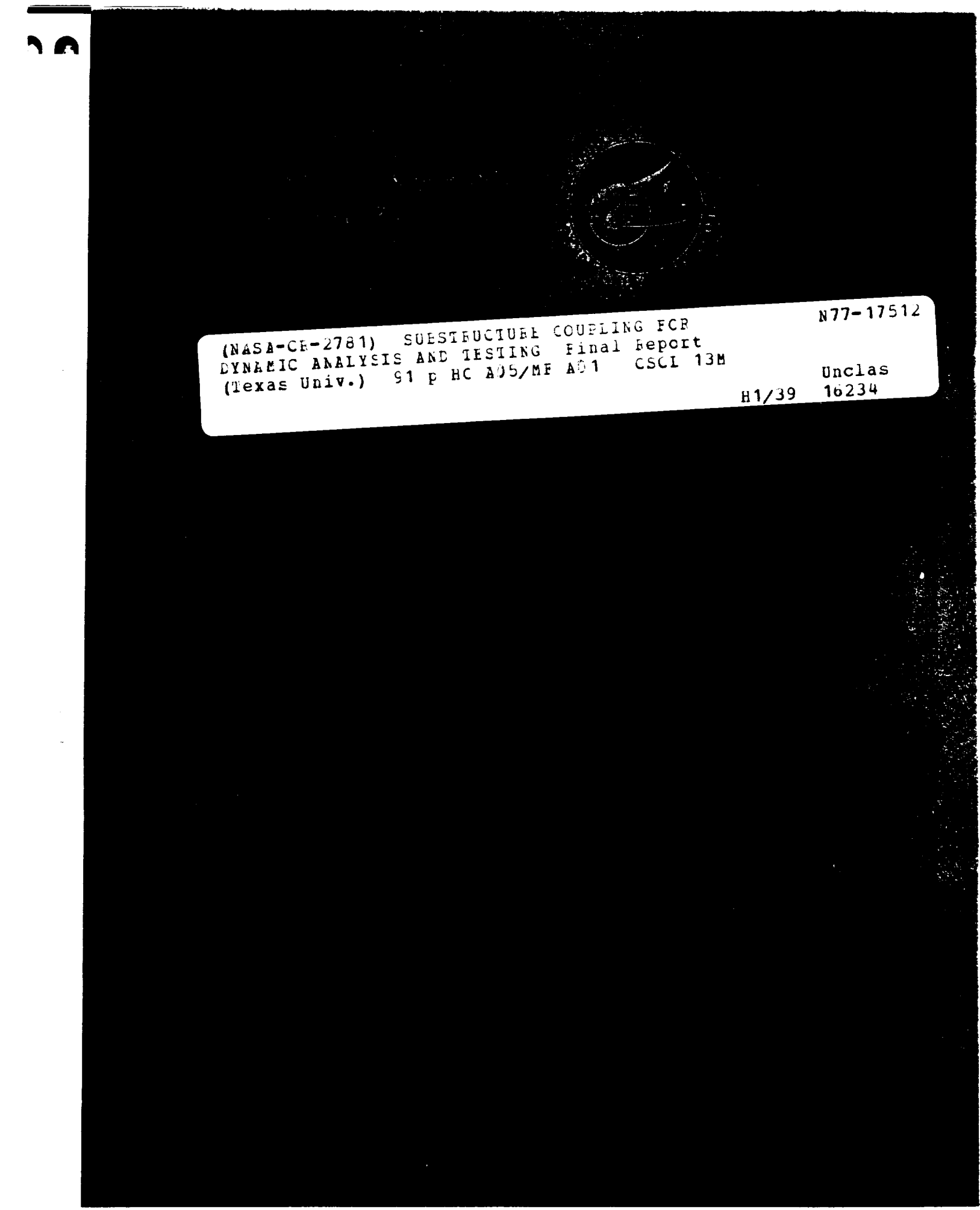

1. Report No.	2. Government Accession No.	3. Recipient's Catalog No.
NASA CR-2781		

4. Title and Subtitle	5. Report Date
SUBSTRUCTURE COUPLING FOR DYNAMIC ANALYSIS AND TESTING	February 1977
	6. Performing Organization Code

7. Author(s)	8. Performing Organization Report No.
Roy R. Craig, Jr., and Ching-Jone Chang	

9. Performing Organization Name and Address	10. Work Unit No.
University of Texas at Austin Austin, Texas 78712	506-17-31-01
	11. Contract or Grant No. NSG 1001

12. Sponsoring Agency Name and Address	13. Type of Report and Period Covered
National Aeronautics and Space Administration Washington, DC 20546	Contractor Report
	14. Sponsoring Agency Code

15. Supplementary Notes

Final Report

Langley technical monitor: Robert W. Fralich

16. Abstract

Fixed-interface and free-interface methods of substructure coupling for dynamic analysis are treated. Three methods for reducing interface coordinates required by fixed-interface methods (Hurty, Craig-Bampton) are introduced. Reduction of substructure interface coordinates is compared with reduction of substructure normal mode coordinates. The free-interface methods of representation of substructures due to MacNeal and Rubin are discussed. Methods of coupling these free-interface substructure models are derived, and results obtained with these methods are compared to results obtained using the Craig-Bampton fixed-interface method and using Hou's free-interface method. The relationship of substructure analysis to substructure testing is discussed briefly.

17. Key Words (Suggested by Author(s))	18. Distribution Statement
Structural Dynamics Vibrations Substructure coupling	Unclassified - Unlimited Subject Category 39

19. Security Classif. (of this report)	20. Security Classif. (of this page)	21. No. of Pages	22. Price*
UNCLASSIFIED	UNCLASSIFIED	89	$4.75

* For sale by the National Technical Information Service, Springfield, Virginia 22161

SUBSTRUCTURE COUPLING FOR DYNAMIC ANALYSIS AND TESTING

Roy R. Craig, Jr.*; and Ching-Jone Chang†
The University of Texas at Austin

SUMMARY

Substructure coupling methods may be classified as fixed-interface methods, free-interface methods, or hybrid methods, depending on whether the modes used are determined with substructure interfaces fully restrained, free of restraint, or partially restrained.

In the present report three methods are presented for reducing the number of interface coordinates required by fixed interface methods. These are: Ritz reduction, Guyan reduction, and modal reduction. Example solutions are given to illustrate these three methods, and procedures for estimating convergence properties of the methods are described.

Also presented in the report is a study of a class of free-interface methods. The methods described appear to be significantly more accurate than the free-interface methods of Hou and Goldman and to be particularly useful when experimental verification of the analytical model is required. The substructure equations and coupling equations are developed, and example problems are presented which compare the accuracy of the present methods with other free-interface methods and with fixed-interface methods.

*Associate Professor, Aerospace Engineering and Engineering Mechanics
†Graduate Student, Engineering Mechanics

INTRODUCTION

Substructure coupling methods may be employed when (1) the number of coordinates in a dynamic analysis needs to be reduced, or (2) when analysis or testing of a structure needs to be done separately on different portions of the structure. Substructure coupling methods generally employ coordinate transformations where the generalized coordinates of substructures are defined by Ritz-type modes. In most cases some, or all, of the generalized coordinates are defined by a set of substructure free vibration modes. The substructure coupling methods may be classified as fixed-interface methods, free-interface methods, or hybrid methods depending on whether the modes are determined with the substructure interfaces fully restrained, free of restraint, or partially restrained.

The primary focus of the research described in the present report is on methods for reducing the number of interface coordinates required by fixed-interface substructure coupling methods. The fixed-interface method developed by Hurty (ref. 1) and refined by Craig and Bampton (ref. 2) requires that all of the original interface displacement coordinates be retained in the final coupled structure. Benfield, Bodley, and Morosow (ref. 3) conducted a study comparing the accuracy of several substructure coupling procedures. Figure 1 shows some of the results obtained in reference 3. Although the various methods were only applied to one structure, the results of this limited study indicated that the fixed interface method of Hurty and the equivalent Craig-Bampton method generally produced the most accurate solutions for a given number of degrees of freedom. Slightly better accuracy was

achieved by methods introduced by Benfield and Hruda (ref. 4) but these latter methods suffer the disadvantage that the substructure modes of one substructure are not independent of the other substructures. Benfield, et. al. (ref. 3) suggest that a drawback to the Hurty method (and Craig-Bampton method) is the requirement that all interface displacement coordinates, i.e., constraint modes, must be retained in the final coupled structure. It is suggested that this might restrict the number of component, or substructure, normal modes retained in the coupled structure. It is the purpose of this report, therefore, to describe three methods for reducing the number of interface coordinates in the final system model. Reference 5 presents additional information concerning these three methods.

A secondary purpose of this report is concerned with improving the accuracy obtainable from free-interface substructure coupling methods. Figure 1, taken from reference 3, indicates that the two free-interface methods, Hou's method and Goldman's method, produce frequencies much less accurate than those produced by fixed-interface methods for a comparable number of system degrees of freedom.

Subsequent to the appearance of reference 3, Rubin (ref. 6) presented a paper describing a class of free-interface methods similar to ones described previously by MacNeal (ref. 7) and Klosterman (ref. 8). Although Rubin went into considerable detail to describe how to represent individual unconstrained (i.e., possessing rigid-body freedom) substructures, he did not fully develop the substructure coupling procedures or present any examples of multi-substructure systems.

Rubin (ref. 6) stressed the fact that, when experimental verification

of analytical models is required, the class of free-interface substructure methods which he presented are much more attractive than are fixed-interface substructure methods.

Since the methods presented by Rubin appeared to have the potential for producing substructure coupling results of acceptable accuracy and appeared to be compatible with state-of-the-art dynamic testing procedures, it was decided that the initial effort along the lines of improving free-interface methods should be directed toward further development of the methods suggested by Rubin. Rubin's own work (ref. 6) treats only unconstrained substructures. The only example presented is for a single substructure represented by a continuous (i.e., partial differential equation) model. In the present report the theory is presented first for constrained substructures, in order that the concepts may be presented first in the simplest form possible. Also, in the present report only discrete models (i.e., matrix ordinary differential equations) are employed, since these are the ones employed to model practical structures. Finally, the present report presents detailed equations for coupling substructures and presents example problems in which results obtained by Rubin-type methods are compared with results obtained by other methods (Hou, Craig-Bampton).

FIXED INTERFACE METHODS WITH REDUCTION OF INTERFACE COORDINATES

In this part of the report three methods are derived for reducing the number of interface coordinates required for fixed-interface substructure methods. Examples are also presented to assess the accuracy of the derived methods.

Substructure Equations

For a typical substructure, the equations of motion, assuming linear viscous damping, may be written

$$m\ddot{x} + c\dot{x} + kx = f \tag{1}$$

For undamped, free vibration, the equations reduce to

$$m\ddot{x} + kx = f \tag{2}$$

where f contains forces at junction (interface) coordinates in the coupled structure.

In most substructure coupling methods the original substructure physical coordinates are expressed, after the manner of Ritz, in terms of a set of substructure generalized coordinates. In the method of Craig and Bampton (ref. 2) these substructure generalized coordinates consist of a set of junction, or interface, coordinates and a set of normal mode coordinates. These normal modes are obtained with all junction coordinates fully restrained.

Equation (2) may be partitioned to give

$$\begin{bmatrix} m_{ii} & m_{ij} \\ m_{ji} & m_{jj} \end{bmatrix} \begin{Bmatrix} \ddot{x}_i \\ \ddot{x}_j \end{Bmatrix} + \begin{bmatrix} k_{ii} & k_{ij} \\ k_{ji} & k_{jj} \end{bmatrix} \begin{Bmatrix} x_i \\ x_j \end{Bmatrix} = \begin{Bmatrix} 0 \\ f_j \end{Bmatrix} \tag{3}$$

where x_i contains the "interior", or non-interface, physical coordinates and x_j contains the "junction", or interface coordinates. Figure 2 shows interior nodes and junction nodes of two adjacent substructures.

Since the normal modes are to be obtained with $x_j = 0$, Eq. (3) reduces to

$$m_{ii}\, \ddot{x}_i + k_{ii}\, x_i = 0 \quad . \tag{4}$$

The mode shapes, ϕ_n, can be assumed to be normalized so that

$$\phi_n^T\, m\, \phi_n = 1 \tag{5}$$

$$\phi_n^T\, k\, \phi_n = \lambda_n^2 \tag{6}$$

and the mode shapes collected to form the respective columns of a modal matrix Φ_{ii}. The substructure "frequency" has been designated λ to distinguish it from the system frequency ω. Later, the modal matrix will be partitioned so that some of the modes are kept in the final analysis while other modes are reduced out.

If there were no loads (including inertia loads) at the interior coordinates of the substructure, the static displacement would be given by

$$\begin{bmatrix} k_{ii} & k_{ij} \\ k_{ji} & k_{jj} \end{bmatrix} \begin{Bmatrix} x_i \\ x_j \end{Bmatrix} = \begin{Bmatrix} 0 \\ f_j \end{Bmatrix} \tag{7}$$

Displacements x_j of the junction coordinates would produce displacements of the interior coordinates as given by the upper partition of Eq. (7), namely

$$x_i = (- k_{ii}^{-1} k_{ij}) x_j \tag{8}$$

or

$$x_i = \Phi_{ij} x_j \tag{9}$$

The components of the transformation matrix Φ_{ij} can be obtained by solving the equation

$$k_{ii} \Phi_{ij} = - k_{ij} \tag{10}$$

A substructure coordinate transformation may be defined now by

$$x \equiv \begin{Bmatrix} x_i \\ x_j \end{Bmatrix} = \begin{bmatrix} \Phi_{ii} & \Phi_{ij} \\ 0 & I \end{bmatrix} \begin{Bmatrix} p_i \\ p_j \end{Bmatrix} \tag{11}$$

or

$$x = \Phi p \tag{12}$$

The equations of motion may be transformed to the new substructure generalized coordinate system as follows:

$$\bar{m} \ddot{p} + \bar{c} \dot{p} + \bar{k} p = g \tag{13}$$

where

$$\begin{aligned} \bar{m} &= \Phi^T m \Phi \\ \bar{c} &= \Phi^T c \Phi \\ \bar{k} &= \Phi^T k \Phi \\ g &= \Phi^T f \end{aligned} \tag{14}$$

The transformed matrices may be written in more explicit form through the use of Eqs. (11) and (14). Thus,

$$\bar{m} = \begin{bmatrix} \bar{m}_{ii} & \bar{m}_{ij} \\ \bar{m}_{ji} & \bar{m}_{jj} \end{bmatrix}$$

$$\bar{c} = \begin{bmatrix} \bar{c}_{ii} & \bar{c}_{ij} \\ \bar{c}_{ji} & \bar{c}_{jj} \end{bmatrix} \tag{15}$$

$$\bar{k} = \begin{bmatrix} \bar{k}_{ii} & 0 \\ 0 & \bar{k}_{jj} \end{bmatrix}$$

The null partitions of $\bar{k}$ result from the transformation imposed by Eq. (10). The remaining submatrices are given by

$$
\begin{aligned}
\bar{m}_{ii} &= I_i \\
\bar{m}_{ij} &= \bar{m}_{ji}^T = \Phi_{ii}^T (m_{ii}\Phi_{ij} + m_{ij}) \\
\bar{m}_{jj} &= m_{jj} + \Phi_{ij}^T (m_{ii}\Phi_{ij} + m_{ij}) + m_{ji}\Phi_{ij} \\
\bar{k}_{ii} &= [\lambda^2] \\
\bar{k}_{jj} &= k_{jj} + k_{ji}\Phi_{ij} \\
\bar{c}_{ii} &= \Phi_{ii}^T c_{ii} \Phi_{ii} \\
\bar{c}_{ij} &= \bar{c}_{ji}^T = \Phi_{ii}^T (c_{ii}\Phi_{ij} + c_{ij}) \\
\bar{c}_{jj} &= c_{jj} + \Phi_{ij}^T (c_{ii}\Phi_{ij} + c_{ij}) + c_{ji}\Phi_{ij}
\end{aligned}
\qquad (16)
$$

Coupled System Equations

In discussing the coupled system, we will consider two substructures, "A" and "B". Extension to more substructures is straightforward. The total set of system generalized coordinates is

$$q \equiv \begin{Bmatrix} q_i \\ q_j \end{Bmatrix} \tag{17}$$

where q_i is a collection of all substructure (interior) normal mode coordinates and q_j is a set of all junction coordinates. Although it is common practice at this point to reduce the number of coordinates by including only selected modes from each substructure, we will assume that all modes are retained for the time being and will treat the reduction of coordinates question in a later section.

The substructure coordinates are related to the system coordinates by "label" submatrices, which simply identify substructure coordinates with the appropriate system coordinates. This is a formal expression of the "direct stiffness" procedure for assembling system matrices from element matrices. Thus,

$$p \equiv \begin{Bmatrix} p_{iA} \\ p_{jA} \\ p_{iB} \\ p_{jB} \end{Bmatrix} = \begin{bmatrix} L_{iA} & 0 & 0 \\ 0 & 0 & L_{jA} \\ 0 & L_{iB} & 0 \\ 0 & 0 & L_{jB} \end{bmatrix} \begin{Bmatrix} q_{iA} \\ q_{iB} \\ q_j \end{Bmatrix} \tag{18}$$

or

$$p = L\,q \quad . \tag{19}$$

The system matrices are obtained by direct stiffness assembly procedures using the labelling information of Eq. (18). The resulting system equations may be written

$$M\,\ddot{q} + C\,\dot{q} + K\,q = F \quad . \tag{20}$$

In partitioned form the equations of motion for free vibration of the undamped coupled system are

$$\left[\begin{array}{ccc} M_{iiA} & 0 & M_{ijA} \\ 0 & M_{iiB} & M_{ijB} \\ M_{jiA} & M_{jiB} & M_{jjA}+M_{jjB} \end{array}\right] \left\{\begin{array}{c} \ddot{q}_{iA} \\ \ddot{q}_{iB} \\ \ddot{q}_{j} \end{array}\right\} + \left[\begin{array}{ccc} K_{iiA} & 0 & 0 \\ 0 & K_{iiB} & 0 \\ 0 & 0 & K_{jjA}+K_{jjB} \end{array}\right] \left\{\begin{array}{c} q_{iA} \\ q_{iB} \\ q_{j} \end{array}\right\} = \left\{\begin{array}{c} 0 \\ 0 \\ 0 \end{array}\right\} \tag{21}$$

For the undamped free vibration problem we can take

$$q(t) = Q \cos(\omega t) \tag{22}$$

where Q is a vector of amplitudes only. The resulting eigenvalue problem has the form

$$\begin{bmatrix} K_{ii} & 0 \\ 0 & K_{jj} \end{bmatrix} \begin{Bmatrix} Q_i \\ Q_j \end{Bmatrix} - \omega^2 \begin{bmatrix} M_{ii} & M_{ij} \\ M_{ji} & M_{jj} \end{bmatrix} \begin{Bmatrix} Q_i \\ Q_j \end{Bmatrix} = \begin{Bmatrix} 0 \\ 0 \end{Bmatrix} \qquad (23)$$

where the substructure normal mode coordinates have been combined into a single vector $q_i = Q_i \cos(\omega t)$.

In the following sections we will discuss the effect of reducing out some of the substructure normal mode coordinates and/or some of the junction coordinates.

Reduction of Coordinates

One of the primary reasons for adopting a substructure method for solving structural dynamics problems is to reduce the number of degrees of freedom which must be employed in the dynamic analysis. The truncation of substructure normal modes in a fixed-interface substructure coupling analysis has been studied by Hurty (ref. 9), Benfield, Bodley, and Morosow (ref. 3), and others. For completeness, this procedure is described below. The reduction of junction (interface) coordinates has apparently not been considered previously. Three possible methods for reducing junction coordinates are introduced in succeeding sections. These are referred to as modal reduction, Guyan reduction, and Ritz reduction.

Reduction of substructure normal mode coordinates. - For considering reduction of normal mode coordinates we can partition Q_i in Eq. (23), giving

$$\begin{bmatrix} K_{aa} & 0 & 0 \\ 0 & K_{bb} & 0 \\ 0 & 0 & K_{jj} \end{bmatrix} \begin{Bmatrix} Q_a \\ Q_b \\ Q_j \end{Bmatrix} - \omega^2 \begin{bmatrix} M_{aa} & 0 & M_{aj} \\ 0 & M_{bb} & M_{bj} \\ M_{ja} & M_{jb} & M_{jj} \end{bmatrix} \begin{Bmatrix} Q_a \\ Q_b \\ Q_j \end{Bmatrix} = \begin{Bmatrix} 0 \\ 0 \\ 0 \end{Bmatrix} \tag{24}$$

where coordinates Q_a will be retained and coordinates Q_b will be reduced out. The second row-partition of Eq. (24) may be written

$$(K_{bb} - \omega^2 M_{bb})\, Q_b = \omega^2 M_{bj}\, Q_j \tag{25}$$

or

$$Q_b = \omega^2 \left(I - \omega^2 K_{bb}^{-1} M_{bb}\right)^{-1} K_{bb}^{-1} M_{bj} Q_j \tag{26}$$

Consider the eigenvalue problem

$$\left(K_{bb} - \lambda^2 M_{bb}\right) Q_b = 0 \tag{27}$$

i.e., the eigenvalue problem associated with the substructure modes to be reduced out. The frequencies of these substructure modes are called λ_n to distinguish them from frequencies ω of the coupled system. Recall that the modes are normalized so that $M_{bb} = I$ and K_{bb} is a diagonal matrix containing λ_n^2's. Thus, Eq. (26) takes the form

$$Q_b = \left[\frac{(\omega/\lambda_n)^2}{1 - (\omega/\lambda_n)^2}\right] M_{bj} Q_j \tag{28}$$

Let λ_1 be the lowest frequency among the eigenvalues of Eq. (27), i.e., the lowest frequency of a mode which is to be reduced out. If the range of system frequencies, ω, of interest is such that

$$\omega/\lambda_1 << 1 \tag{29}$$

the zeroth-order approximation to Q_b is

$$Q_b = 0 \tag{30}$$

i.e., the modes associated with Q_b can just be eliminated. The reduced eigenvalue problem is simply

$$\begin{bmatrix} K_{aa} & 0 \\ 0 & K_{jj} \end{bmatrix} \begin{Bmatrix} Q_a \\ Q_j \end{Bmatrix} - \omega^2 \begin{bmatrix} M_{aa} & M_{aj} \\ M_{ja} & M_{jj} \end{bmatrix} \begin{Bmatrix} Q_a \\ Q_j \end{Bmatrix} = \begin{Bmatrix} 0 \\ 0 \end{Bmatrix} \tag{31}$$

An iterative procedure for improving frequencies and mode shapes of the system could be based on using the zero-order approximate values of ω in Eq. (28). Kuhar and Stahle (ref. 10) proposed a "dynamic transformation" procedure which essentially consists of defining Q_b in terms of Q_j through Eq. (28) using a pre-selected transformation frequency, ρ, instead of the (unknown) system frequency ω. However, M_{bj} involves mode shapes of the deleted modes, and hence this procedure requires that such modes be obtained in the original substructure eigensolutions.

Examples will be presented in a later section to compare the effectiveness of reducing out substructure normal modes with the effectiveness of reducing out junction coordinates.

Modal reduction of junction coordinates. - This section will introduce the technique of modal reduction of junction coordinates. Consider the eigenvalue problem that would be obtained from Eq. (23) by constraining the substructure normal mode coordinates and allowing motion of junction coordinates, i.e.,

$$(K_{jj} - \delta^2 M_{jj}) Q_j = 0 \tag{32}$$

It may be noted that this corresponds to using Guyan reduction to reduce out all interior coordinates. The frequencies of these "junction modes" will be

called δ to distinguish them from system frequencies, ω, and substructure frequencies, λ. Let the junction modes form a modal matrix Ψ_j, which has the form

$$\Psi_j = [\Psi_{jc} \; \Psi_{jd}] \tag{33}$$

where the modes Ψ_{jc} will be kept and modes Ψ_{jd} will be reduced out. Assume that the modes are normalized with respect to M_{jj} in the usual fashion. Now let

$$Q_j = [\Psi_{jc} \; \Psi_{jd}] \begin{Bmatrix} \bar{Q}_c \\ \bar{Q}_d \end{Bmatrix} \tag{34}$$

Then,

$$Q \equiv \begin{Bmatrix} Q_i \\ Q_j \end{Bmatrix} = \begin{bmatrix} I & 0 & 0 \\ 0 & \Psi_{jc} & \Psi_{jd} \end{bmatrix} \begin{Bmatrix} \bar{Q}_i \\ \bar{Q}_c \\ \bar{Q}_d \end{Bmatrix} \tag{35}$$

or

$$Q = \Psi \bar{Q} \tag{36}$$

Transformations of the form

$$\bar{K} = \Psi^T K \Psi \tag{37}$$

transform Eq. (23) to the form

$$\begin{bmatrix} \bar{K}_{ii} & 0 & 0 \\ 0 & \bar{K}_{cc} & 0 \\ 0 & 0 & \bar{K}_{dd} \end{bmatrix} \begin{Bmatrix} \bar{Q}_i \\ \bar{Q}_c \\ \bar{Q}_d \end{Bmatrix} - \omega^2 \begin{bmatrix} \bar{M}_{ii} & \bar{M}_{ic} & \bar{M}_{id} \\ \bar{M}_{ci} & \bar{M}_{cc} & 0 \\ \bar{M}_{di} & 0 & \bar{M}_{dd} \end{bmatrix} \begin{Bmatrix} \bar{Q}_i \\ \bar{Q}_c \\ \bar{Q}_d \end{Bmatrix} = \begin{Bmatrix} 0 \\ 0 \\ 0 \end{Bmatrix} \tag{38}$$

The zeros in the c-d coupling terms are due to orthogonality of the junction modes. The submatrices in Eq. (38) are obtained from the equations

$$\begin{aligned} \bar{K}_{ii} &= K_{ii} \\ \bar{K}_{cc} &= \Psi_{jc}^T K_{jj} \Psi_{jc} = \lceil \delta_c^2 \rfloor \\ \bar{K}_{dd} &= \Psi_{jd}^T K_{jj} \Psi_{jd} = \lceil \delta_d^2 \rfloor \\ \bar{M}_{ii} &= I_i \\ \bar{M}_{ic} &= M_{ci}^T = M_{ij} \Psi_{jc} \\ \bar{M}_{id} &= \bar{M}_{di}^T = M_{ij} \Psi_{jd} \\ \bar{M}_{cc} &= I_c \\ \bar{M}_{dd} &= I_d \end{aligned} \tag{39}$$

Let Eq. (38) be written as two equations, namely

$$\begin{bmatrix} \bar{K}_{ii} & 0 \\ 0 & \bar{K}_{cc} \end{bmatrix} \begin{Bmatrix} \bar{Q}_i \\ \bar{Q}_c \end{Bmatrix} - \omega^2 \begin{bmatrix} \bar{M}_{ii} & \bar{M}_{ic} \\ \bar{M}_{ci} & \bar{M}_{cc} \end{bmatrix} \begin{Bmatrix} \bar{Q}_i \\ \bar{Q}_c \end{Bmatrix} - \omega^2 \begin{bmatrix} \bar{M}_{id} \\ 0 \end{bmatrix} \bar{Q}_d = \begin{Bmatrix} 0 \\ 0 \end{Bmatrix} \tag{40}$$

and

$$(\bar{K}_{dd} - \omega^2 \bar{M}_{dd}) \bar{Q}_d = \omega^2 \bar{M}_{di} \bar{Q}_i \tag{41}$$

Since, according to Eqs. (39), $\bar{K}_{dd}$ and $\bar{M}_{dd}$ are diagonal, Eq. (41) may be written

$$\bar{Q}_d = W_{dd} \bar{M}_{di} \bar{Q}_i \tag{42}$$

where

$$W_{dd} = \lceil w_n \rfloor \tag{43}$$

is a diagonal matrix whose elements are given by

$$w_n = \frac{\omega^2}{\delta_n^2 - \omega^2} \tag{44}$$

When Eq. (42) is substituted into Eq. (40) the resulting equation may be written

$$\begin{bmatrix} \bar{K}_{ii} & 0 \\ 0 & \bar{K}_{cc} \end{bmatrix} \begin{Bmatrix} \bar{Q}_i \\ \bar{Q}_c \end{Bmatrix} - \omega^2 \begin{bmatrix} (\bar{M}_{ii} + \Delta M_{ii}) & \bar{M}_{ic} \\ \bar{M}_{ci} & \bar{M}_{cc} \end{bmatrix} \begin{Bmatrix} \bar{Q}_i \\ \bar{Q}_c \end{Bmatrix} = \begin{Bmatrix} 0 \\ 0 \end{Bmatrix} \tag{45}$$

where

$$\Delta M_{ii} = \bar{M}_{id} W_{dd} \bar{M}_{di} = \sum_n w_n M_{ij} \psi_n \psi_n^T M_{ji} \tag{46}$$

in which ψ_n is the junction mode corresponding to δ_n^2 .

The derivation of "modal participation factors," which provide an estimate of the contribution of each junction mode to the solution of Eq. (45) proceeds along lines similar to the procedure employed by Hurty in reference 9 for discussing truncation of substructure normal modes.

First a "base problem" is defined by setting $\Delta M_{ii} = 0$ in Eq. (45) or, equivalently, setting $\bar{Q}_d = 0$ in Eq. (40), giving

$$\begin{bmatrix} \bar{K}_{ii} & 0 \\ 0 & \bar{K}_{cc} \end{bmatrix} \begin{Bmatrix} \bar{Q}_{io} \\ \bar{Q}_{co} \end{Bmatrix} - \omega_o^2 \begin{bmatrix} \bar{M}_{ii} & \bar{M}_{ic} \\ \bar{M}_{ci} & \bar{M}_{cc} \end{bmatrix} \begin{Bmatrix} \bar{Q}_{io} \\ \bar{Q}_{co} \end{Bmatrix} = \begin{Bmatrix} 0 \\ 0 \end{Bmatrix} \tag{47}$$

The exact solution of Eq. (38) and the solution of Eq. (47) are related by

$$\omega^2 = \omega_o^2 + \Delta\omega^2 \tag{48}$$

and

$$\bar{Q} = \bar{Q}_o + \Delta Q \tag{49}$$

where

$$\bar{Q}_o = \begin{Bmatrix} \bar{Q}_{io} \\ \bar{Q}_{co} \\ 0 \end{Bmatrix} \tag{50}$$

When Eqs. (47), (48), and (49) are substituted into Eq. (45) and "higher order terms" in $\Delta\omega^2$ are neglected, there results

$$\begin{bmatrix} \bar{K}_{ii} & 0 \\ 0 & \bar{K}_{cc} \end{bmatrix} \begin{Bmatrix} \Delta Q_i \\ \Delta Q_c \end{Bmatrix} - \omega_o^2 \begin{bmatrix} \bar{M}_{ii} & \bar{M}_{ic} \\ \bar{M}_{ci} & \bar{M}_{cc} \end{bmatrix} \begin{Bmatrix} \Delta Q_i \\ \Delta Q_c \end{Bmatrix} - \Delta\omega^2 \begin{bmatrix} \bar{M}_{ii} & \bar{M}_{ic} \\ \bar{M}_{ci} & \bar{M}_{cc} \end{bmatrix} \begin{Bmatrix} \bar{Q}_{io} \\ \bar{Q}_{co} \end{Bmatrix}$$

$$- \omega_o^2 \begin{bmatrix} \Delta M_{ii}(\omega_o) & 0 \\ 0 & 0 \end{bmatrix} \begin{Bmatrix} \bar{Q}_{io} \\ \bar{Q}_{co} \end{Bmatrix} = \begin{Bmatrix} 0 \\ 0 \end{Bmatrix} \tag{51}$$

If Eq. (51) is premultiplied by $[\bar{Q}_{io}^T \ \bar{Q}_{co}^T]$, ΔQ is expanded in terms of the eigenvectors, $\bar{Q}_o$, and proper account is taken of Eq. (47) and orthogonality, there results

$$\frac{\Delta\omega^2}{\omega_o^2} = \frac{-\bar{Q}_{io}^T \Delta M_{ii}(\omega_o) \bar{Q}_{io}}{\begin{Bmatrix} \bar{Q}_{io} \\ \bar{Q}_{co} \end{Bmatrix}^T \begin{bmatrix} \bar{M}_{ii} & \bar{M}_{ic} \\ \bar{M}_{ci} & \bar{M}_{cc} \end{bmatrix} \begin{Bmatrix} \bar{Q}_{io} \\ \bar{Q}_{co} \end{Bmatrix}} \tag{52}$$

If the solution vectors of the base problem are normalized relative to the mass matrix of the base problem the denominator of Eq. (52) becomes unity, so the eigenvalue error is given by

$$\frac{\Delta\omega^2}{\omega_o^2} = -\bar{Q}_{io}^T \Delta M_{ii}(\omega_o) \bar{Q}_{io} \tag{53}$$

But, since ΔM_{ij} can be written as a sum, as shown in Eq. (46), Eq. (53) may be written

$$\frac{\Delta\omega^2}{\omega_o^2} = - \sum_n \frac{\omega_o^2 \left(\bar{Q}_{io}^T M_{ij} \psi_n\right)^2}{\delta_n^2 - \omega_o^2} \tag{54}$$

From Eq. (54) it is clear that modal participation factors can be defined by

$$P_n \equiv \frac{\Delta_n\omega^2}{\omega_o^2} = - \frac{\omega_o^2 \left(\bar{Q}_{io}^T M_{ij} \psi_n\right)^2}{\delta_n^2 - \omega_o^2} \tag{55}$$

Two factors are of interest in determining the value of the modal participation factor: (a) the frequency ratio, ω_o/δ_n , and (b) the mass coupling. If $\omega_o/\delta_n << 1$ the nth junction mode should have little contribution to the frequency of a given system mode. On the other hand, Eq. (55) shows that the coupling of the interior portion of the base problem mode, i.e., $\bar{Q}_{io}$, with the nth junction mode through the original coupling mass matrix M_{ij} is also important. Hence, the modal participation factor given by Eq. (55) should, where possible, be used as a basis for selecting junction modes to be retained.

It is clear from Eq. (55) that the concept of modal participation factor has meaning only in reference to choosing modes which would lead to a maximum improvement upon a given base solution. The question arises, then, as to what should constitute the base problem, i.e., what junction modes belong to Ψ_{jc} in Eq. (34). It would seem that the only rational approach to this problem would be to select a specified number of junction modes using junction

frequency alone as the criterion, i.e., order the junction modes according to frequency and use the modes from the lower end of the frequency spectrum. If there are any rigid-body junction modes, these must be included in the base problem.

In a later section, an example will be presented to illustrate the calculation of modal participation factors.

Guyan reduction of junction coordinates. - In reference 11, Anderson, et. al., applied the method of Guyan reduction to a plate vibration problem and showed that acceptable accuracy of frequencies was maintained even when a large percentage of the coordinates were reduced out. In this section, a similar Guyan reduction will be applied. However, in this case only selected junction coordinates will be reduced out.

Consider again Eq. (23) and partition Q_j into

$$Q_j = \begin{Bmatrix} Q_e \\ \\ Q_f \end{Bmatrix} \tag{56}$$

where the Q_f coordinates are to be reduced out by a Guyan-type reduction. Thus, Eq. (23) may be written

$$\begin{bmatrix} K_{ii} & 0 & 0 \\ 0 & K_{ee} & K_{ef} \\ 0 & K_{fe} & K_{ff} \end{bmatrix} \begin{Bmatrix} Q_i \\ Q_e \\ Q_f \end{Bmatrix} - \omega^2 \begin{bmatrix} M_{ii} & M_{ie} & M_{if} \\ M_{ei} & M_{ee} & M_{ef} \\ M_{fi} & M_{fe} & M_{ff} \end{bmatrix} \begin{Bmatrix} Q_i \\ Q_e \\ Q_f \end{Bmatrix} = \begin{Bmatrix} 0 \\ 0 \\ 0 \end{Bmatrix}$$

Guyan reduction is based on neglecting inertia terms in the third row-partition of Eq. (57) to obtain

$$Q_f = \Psi_{fe} Q_e \tag{58}$$

where

$$\Psi_{fe} = - K_{ff}^{-1} K_{fe} \tag{59}$$

Although there is no established procedure for selecting coordinates to be retained and coordinates to be deleted, i.e., for ordering the Q_j coordinates in Eq. (56), a possible procedure for selecting the coordinates to be retained might be based on magnitudes of the quotient of terms on the diagonal of K_{jj} divided by corresponding terms on the diagonal of M_{jj}, with the coordinates having the smaller k/m values being retained.

The junction coordinate reduction equation, Eq. (59), has the same form as a substructure equation, Eq. (8). The system displacement transformation, based on Eq. (58), is

$$\begin{Bmatrix} Q_i \\ Q_e \\ Q_f \end{Bmatrix} = \begin{bmatrix} I & 0 \\ 0 & I \\ 0 & \Psi_{fe} \end{bmatrix} \begin{Bmatrix} \bar{Q}_i \\ \bar{Q}_e \end{Bmatrix} \tag{60}$$

Note that the coordinates Q_f are reduced out, i.e., approximated by Eq. (58). They are not simply eliminated as were Q_b, Eq. (30), and $\bar{Q}_d$, Eq. (47).

Transformation of Eq. (57) to the reduced set of coordinates $\bar{Q}$ defined by Eq. (60) gives

$$\begin{bmatrix} \bar{K}_{ii} & 0 \\ 0 & \bar{K}_{ee} \end{bmatrix} \begin{Bmatrix} \bar{Q}_i \\ \bar{Q}_e \end{Bmatrix} - \omega^2 \begin{bmatrix} \bar{M}_{ii} & \bar{M}_{ie} \\ \bar{M}_{ei} & \bar{M}_{ee} \end{bmatrix} \begin{Bmatrix} \bar{Q}_i \\ \bar{Q}_e \end{Bmatrix} = \begin{Bmatrix} 0 \\ 0 \end{Bmatrix} \tag{61}$$

where

$$\begin{aligned} \bar{K}_{ii} &= K_{ii} \\ \bar{K}_{ee} &= K_{ee} + K_{ef} \Psi_{fe} \\ \bar{M}_{ii} &= M_{ii} = I_i \\ \bar{M}_{ie} &= \bar{M}_{ei}^T = M_{ie} + M_{if} \Psi_{fe} \\ \bar{M}_{ee} &= M_{ee} + M_{ef} \Psi_{fe} + \Psi_{fe}^T (M_{fe} + M_{ff} \Psi_{fe}) \end{aligned} \tag{62}$$

Note the similarity of the above expressions to those in Eq. (16).

An example of the use of Guyan reduction will be presented in the section on example problems.

Ritz reduction of junction coordinates. - The modal reduction and Guyan reduction of junction coordinates which were presented in the preceeding sections are both special cases of Ritz representation of junction coordinates. There are cases where the nature of the problem might suggest a direct approach of Ritz at either the substructure level or the coupled system level.

We will employ the latter approach, beginning with Eq. (23), repeated here for convenience.

$$\begin{bmatrix} K_{ii} & 0 \\ 0 & K_{jj} \end{bmatrix} \begin{Bmatrix} Q_i \\ Q_j \end{Bmatrix} - \omega^2 \begin{bmatrix} M_{ii} & M_{ij} \\ M_{ji} & M_{jj} \end{bmatrix} \begin{Bmatrix} Q_i \\ Q_j \end{Bmatrix} = \begin{Bmatrix} 0 \\ 0 \end{Bmatrix} \tag{23}$$

Let the junction coordinates be expanded in terms of a set of Ritz vectors according to the equation

$$Q_j = \Psi_{jg} \bar{Q}_g \tag{63}$$

where notation similar to that of the preceding sections is employed. The matrix Ψ_{jg} is rectangular, $(n_j > n_g)$, since the number of coordinates is to be reduced by this Ritz expansion. The columns of Ψ_{jg} represent the displacement of junction coordinates in each of the Ritz "modes".

$$\begin{Bmatrix} Q_i \\ Q_j \end{Bmatrix} = \begin{bmatrix} I & 0 \\ 0 & \Psi_{jg} \end{bmatrix} \begin{Bmatrix} \bar{Q}_i \\ \bar{Q}_g \end{Bmatrix} \tag{64}$$

As before, this can be represented by

$$Q = \Psi \bar{Q} \tag{65}$$

and the stiffness matrix becomes

$$\bar{K} = \Psi^T K \Psi \tag{66}$$

Then the system equation, Eq. (23), is transformed into

$$\begin{bmatrix} \bar{K}_{ii} & 0 \\ 0 & \bar{K}_{gg} \end{bmatrix} \begin{Bmatrix} \bar{Q}_i \\ \bar{Q}_g \end{Bmatrix} - \omega^2 \begin{bmatrix} \bar{M}_{ii} & \bar{M}_{ig} \\ \bar{M}_{gi} & \bar{M}_{gg} \end{bmatrix} \begin{Bmatrix} \bar{Q}_i \\ \bar{Q}_g \end{Bmatrix} = \begin{Bmatrix} 0 \\ 0 \end{Bmatrix} \tag{67}$$

where

$$\begin{aligned} \bar{K}_{ii} &= K_{ii} \\ \bar{K}_{gg} &= \Psi_{jg}^T K_{jj} \Psi_{jg} \\ \bar{M}_{ii} &= M_{ii} = I_i \\ \bar{M}_{ig} &= \bar{M}_{gi}^T = M_{ij} \Psi_{jg} \\ \bar{M}_{gg} &= \Psi_{jg}^T M_{jj} \Psi_{jg} \end{aligned} \tag{68}$$

where $\bar{K}_{ii}$ and $\bar{M}_{ii}$ are diagonal.

The use of Eq. (67) for reduction of junction coordinates will be illustrated in the section on example problems.

It is possible to write expressions for error analysis, or for modal participation factor analysis, for the general case of Ritz representation of junction coordinates. First, Eq. (63) will be expanded by assuming that one or more Ritz vectors (or modes) are to be added in Eq. (63), with the set Ψ_{jg} forming the "base problem" and Ψ_{jh} being the added vectors. Thus,

$$Q_j = [\Psi_{jg} \; \Psi_{jh}] \begin{Bmatrix} \bar{Q}_g \\ \bar{Q}_h \end{Bmatrix} \tag{69}$$

This gives a base problem similar to Eq. (67), namely

$$\begin{bmatrix} \bar{K}_{ii} & 0 \\ 0 & \bar{K}_{gg} \end{bmatrix} \begin{Bmatrix} \bar{Q}_{io} \\ \bar{Q}_{go} \end{Bmatrix} - \omega_o^2 \begin{bmatrix} \bar{M}_{ii} & \bar{M}_{ig} \\ \bar{M}_{gi} & \bar{M}_{gg} \end{bmatrix} \begin{Bmatrix} \bar{Q}_{io} \\ \bar{Q}_{go} \end{Bmatrix} = \begin{Bmatrix} 0 \\ 0 \end{Bmatrix} \tag{70}$$

and an "augmented problem" of the form

$$\begin{bmatrix} \bar{K}_{ii} & 0 & 0 \\ 0 & \bar{K}_{gg} & \bar{K}_{gh} \\ 0 & \bar{K}_{hg} & \bar{K}_{hh} \end{bmatrix} \begin{Bmatrix} \bar{Q}_i \\ \bar{Q}_g \\ \bar{Q}_h \end{Bmatrix} - \omega^2 \begin{bmatrix} \bar{M}_{ii} & \bar{M}_{ig} & \bar{M}_{ih} \\ \bar{M}_{gi} & \bar{M}_{gg} & \bar{M}_{gh} \\ \bar{M}_{hi} & \bar{M}_{hg} & \bar{M}_{hh} \end{bmatrix} \begin{Bmatrix} \bar{Q}_i \\ \bar{Q}_g \\ \bar{Q}_h \end{Bmatrix} = \begin{Bmatrix} 0 \\ 0 \\ 0 \end{Bmatrix} \tag{71}$$

where, in addition to terms defined by Eq. (68),

$$\begin{aligned} \bar{K}_{gh} &= \bar{K}_{hg}^T = \Psi_{jg}^T K_{jj} \Psi_{jh} \\ \bar{K}_{hh} &= \Psi_{jh}^T K_{jj} \Psi_{jh} \\ M_{ih} &= M_{hi}^T = M_{ij} \Psi_{jh} \\ \bar{M}_{gh} &= \bar{M}_{hg}^T = \Psi_{jg}^T M_{jj} \Psi_{jh} \\ \bar{M}_{hh} &= \Psi_{jh}^T K_{jj} \Psi_{jh} \end{aligned} \tag{72}$$

Equation (71) can be written

$$\begin{bmatrix} \bar{K}_{ii} & 0 \\ 0 & \bar{K}_{gg} \end{bmatrix} \begin{Bmatrix} \bar{Q}_i \\ \bar{Q}_g \end{Bmatrix} - \omega^2 \begin{bmatrix} \bar{M}_{ii} & \bar{M}_{ig} \\ \bar{M}_{gi} & \bar{M}_{gg} \end{bmatrix} \begin{Bmatrix} \bar{Q}_i \\ \bar{Q}_g \end{Bmatrix} + \begin{bmatrix} (0 - \omega^2 \bar{M}_{ih}) \\ (\bar{K}_{gh} - \omega^2 \bar{M}_{gh}) \end{bmatrix} \bar{Q}_h = \begin{Bmatrix} 0 \\ 0 \end{Bmatrix} \tag{73}$$

together with

$$\bar{Q}_h = - [\bar{K}_{hh} - \omega^2 \bar{M}_{hh}]^{-1} [(- \omega^2 \bar{M}_{hi}) (\bar{K}_{hg} - \omega^2 \bar{M}_{hg})] \begin{Bmatrix} \bar{Q}_i \\ \bar{Q}_g \end{Bmatrix} \tag{74}$$

There might be instances where the matrix to be inverted in Eq. (74) is singular, but this would simply mean that the Ritz vector causing the singularity is very important at the given frequency ω, since this would imply a very large $\bar{Q}_h$. The matrix inversion in Eq. (74) leads to the definition of w_n in Eq. (44) when junction modes are used as the Ritz vectors.

Equations (73) and (74) may be combined to give

$$\begin{bmatrix} \bar{K}_{ii} & 0 \\ 0 & \bar{K}_{gg} \end{bmatrix} \begin{Bmatrix} \bar{Q}_i \\ \bar{Q}_g \end{Bmatrix} - \omega^2 \begin{bmatrix} \bar{M}_{ii} & \bar{M}_{ig} \\ \bar{M}_{gi} & \bar{M}_{gg} \end{bmatrix} \begin{Bmatrix} \bar{Q}_i \\ \bar{Q}_g \end{Bmatrix}$$

$$- \begin{bmatrix} (0 \quad - \omega^2 \bar{M}_{ih}) \\ (\bar{K}_{gh} - \omega^2 \bar{M}_{gh}) \end{bmatrix} \left[\bar{K}_{hh} - \omega^2 \bar{M}_{hh}\right]^{-1} \begin{bmatrix} (0 \quad - \omega^2 \bar{M}_{ih}) \\ (\bar{K}_{gh} - \omega^2 \bar{M}_{gh}) \end{bmatrix}^T \begin{Bmatrix} \bar{Q}_i \\ \bar{Q}_g \end{Bmatrix} = \begin{Bmatrix} 0 \\ 0 \end{Bmatrix} \tag{75}$$

To simplify notation, let Eq. (75) be written

$$\begin{bmatrix} \bar{K}_{ii} & 0 \\ 0 & \bar{K}_{gg} \end{bmatrix} \begin{Bmatrix} \bar{Q}_i \\ \bar{Q}_g \end{Bmatrix} - \omega^2 \begin{bmatrix} \bar{M}_{ii} & \bar{M}_{ig} \\ \bar{M}_{gi} & \bar{M}_{gg} \end{bmatrix} \begin{Bmatrix} \bar{Q}_i \\ \bar{Q}_g \end{Bmatrix} - \begin{bmatrix} S_{ii} & S_{ig} \\ S_{gi} & S_{gg} \end{bmatrix} \begin{Bmatrix} \bar{Q}_i \\ \bar{Q}_g \end{Bmatrix} = \begin{Bmatrix} 0 \\ 0 \end{Bmatrix} \tag{76}$$

where

$$\begin{aligned} S_{ii} &= \omega^4 \bar{M}_{ih} S_{hh} \bar{M}_{hi} \\ S_{ig} &= S_{gi}^T = -\omega^2 \bar{M}_{ih} S_{hh} (\bar{K}_{hg} - \omega^2 \bar{M}_{hg}) \\ S_{gg} &= (\bar{K}_{gh} - \omega^2 \bar{M}_{gh}) S_{hh} (\bar{K}_{hg} - \omega^2 \bar{M}_{hg}) \end{aligned} \tag{77}$$

where

$$S_{hh} = (\bar{K}_{hh} - \omega^2 \bar{M}_{hh})^{-1} \tag{78}$$

Let the solution of the "augmented problem," Eq. (71), and the solution of the "base problem," Eq. (70), be related by

$$\begin{aligned} \omega^2 &= \omega_o^2 + \Delta\omega^2 \\ \bar{Q} &= \bar{Q}_o + Q \end{aligned} \tag{79}$$

and assume that the eigenvectors of the base problem are normalized on the mass matrix of that problem.

For the case of modal junction coordinates it is easy to simplify the expressions given in Eq. (77) above. Certain assumptions on the expansion of Eq. (77) in powers of ω^2 allow the same to be done here. For purposes of

error analysis, i.e., determining modal participation factors, let it be assumed that the S matrices in Eq. (76) can be approximated by $S(\omega_o)$ giving

$$\begin{bmatrix} \bar{K}_{ii} & 0 \\ 0 & \bar{K}_{gg} \end{bmatrix} \begin{Bmatrix} \Delta Q_i \\ \Delta Q_g \end{Bmatrix} - \omega_o^2 \begin{bmatrix} \bar{M}_{ii} & \bar{M}_{ij} \\ \bar{M}_{gi} & \bar{M}_{gg} \end{bmatrix} \begin{Bmatrix} \Delta Q_i \\ \Delta Q_g \end{Bmatrix}$$

$$- \Delta\omega^2 \begin{bmatrix} \bar{M}_{ii} & \bar{M}_{ig} \\ \bar{M}_{gi} & \bar{M}_{gg} \end{bmatrix} \begin{Bmatrix} \bar{Q}_{io} \\ \bar{Q}_{go} \end{Bmatrix} - \begin{bmatrix} S_{ii}(\omega_o) & S_{ig}(\omega_o) \\ S_{gi}(\omega_o) & S_{gg}(\omega_o) \end{bmatrix} \begin{Bmatrix} \bar{Q}_{io} \\ \bar{Q}_{go} \end{Bmatrix} = \begin{Bmatrix} 0 \\ 0 \end{Bmatrix} \tag{80}$$

Equation (80) is analogous to Eq. (51). Equations (70) and (79) were employed in converting Eq. (76) to Eq. (80). If Eq. (80) is premultiplied by $\bar{Q}_o^T$, ΔQ is expanded in terms of the eigenvectors of the base problem, and proper account is taken of Eq. (70) and orthonormality of the eigenvectors of the base problem, then Eq. (80) reduces to

$$\frac{\Delta\omega^2}{\omega_o^2} = - \frac{1}{\omega_o^2} \begin{Bmatrix} \bar{Q}_{io} \\ \bar{Q}_{go} \end{Bmatrix}^T \begin{bmatrix} S_{ii}(\omega_o) & S_{ig}(\omega_o) \\ S_{gi}(\omega_o) & S_{gg}(\omega_o) \end{bmatrix} \begin{Bmatrix} \bar{Q}_{io} \\ \bar{Q}_{go} \end{Bmatrix} \tag{81}$$

Equation (81) reduces to Eq. (53) for the case of modal junction coordinates.

If a single Ritz vector is used in Ψ_{jh} in Eqs. (72), then Eq. (81) becomes a "modal participation factor" determining the approximate error produced by omission of that vector from the base problem, or, conversely, the approximate improvement of the base problem solution which could be achieved by augmenting the solution by that Ritz vector.

Examples

A limited number of example problems have been solved to illustrate methods for reducing junction coordinates. Three structures were employed in the studies: the two-substructure truss of reference 3, a nine-substructure ring, and a two-substructure grid. The first two structures possess rigid-body freedom; the third is a cantilever structure.

Dimensions have not been given in the example problems of this report since the purpose of the report is to compare relative accuracies of various methods of solving given problems.

Truss examples - modal reduction and Guyan reduction of junction coordinates. - The truss shown in Figure 3 was used by Benfield, et. al. (ref. 3) in their comparison study of substructure coupling methods. Results will be presented for both modal reduction of junction coordinates and Guyan reduction of junction coordinates of this truss.

Table 1 gives results for frequencies of the above truss obtained by the use of modal reduction of junction coordinates. The column headed "Exact" gives results for the coupled structure with all of its original degrees of freedom retained. The remaining results were obtained using substructure coupling with 5 normal modes retained for each substructure, i.e., $N_A = N_B = 5$. The columns headed with $N_j = 6$ give results based on the original Craig-Bampton method, since $N_j = 6$ is the total number of junction coordinates. Since the truss as a whole is free to execute 3 degrees of rigid-body motion, the columns headed $N_j = 3$ give results based on assuming the junction to be rigid, i.e., the 6 junction coordinates must move as a

rigid body. $N_j = 3$ is the smallest number of junction coordinates that may be retained, since it is essential to allow at least rigid-body motion of the junction. The columns headed $N_j = 5$ and $N_j = 4$ give results based on the modal reduction procedure. Note, for example, the frequencies for elastic mode 3. The accuracy of the frequency is not seriously degraded by reduction of junction coordinates until the last stage ($N_j = 3$), but mode 3 does require more than rigid-body behavior from the junction coordinates. The choice of junction modes to be retained was based on junction mode frequency alone.

In Table 1 it may also be noted that the errors in some modes, e.g., elastic modes 7 and 8, are due to truncation of substructure normal modes. The large errors persist even when all six junction coordinates are retained.

Table 2 presents data on substructure normal mode frequencies and junction frequencies. It may be noted that the junction frequencies are the same order of magnitude as the higher-frequency substructure normal modes (e.g., 5th through 10th modes).

It was previously noted that junction mode 4 ($\delta^2 = 0.0182248$) makes a significant contribution to system elastic mode 3 ($\omega^2 = 0.0030508$). Table 3 presents modal participation factor data for this mode so that an assessment may be made of the relative importance of frequency ratio, ω_o/δ_n, and the mass coupling term as they appear in Eq. (55).

The results presented in Table 3 illustrate the fact that both the junction frequency ratio and the mass coupling factor are important in determining the modal participation factor. In the present example it is the low value of the mass coupling factor for junction mode 5 that renders it unimportant in the solution for this particular system mode. The estimated error

Elastic Mode Number	N_j=6, N_A=N_B=5		N_j=5, N_A=N_B=5		N_j=4, N_A=N_B=5		N_j=3, N_A=N_B=5		Exact
	ω^2	% error	ω^2	% error	ω^2	% error	ω^2	% error	ω^2
1	0.0004391	0.00	0.0004391	0.00	0.0004395	0.09	0.0004395	0.09	0.0004391
2	0.0018331	0.01	0.0018331	0.01	0.0018704	2.05	0.0018704	2.05	0.0018329
3	0.0030527	0.06	0.0030568	0.20	0.0030568	0.20	0.0033692	10.44	0.0030508
4	0.0041664	0.18	0.0041664	0.18	0.0042104	1.24	0.0042104	1.24	0.0041589
5	0.0068734	0.22	0.0068734	0.22	0.0068858	0.40	0.0068858	0.40	0.0068585
6	0.0098938	0.17	0.0098938	0.17	0.0100140	1.39	0.0100140	1.39	0.0098770
7	0.0126051	10.61	0.0126051	10.61	0.0126522	11.02	0.0126522	11.02	0.0113959
8	0.0144412	18.02	0.0144475	18.07	0.0144475	18.07	0.0144500	18.09	0.0122362
9	0.0161327	7.05	0.0161327	7.05	0.0163082	8.22	0.0163082	8.22	0.0150701
10	0.0246411	58.82	0.0246411	58.82	0.0257599	66.04	0.0257599	66.04	0.0155146
11	0.0361008	x	0.0407582	x	0.0407582	x	———	———	0.0174052
12	0.0506162	x	0.1030503	x	———	———	———	———	0.0200979
13	0.1030503	x	———	———	———	———	———	———	0.0215105

Table 1. Frequencies of 2-Component Benfield Truss with Modal Interface Reductions

Type / Mode	Component A	Component B	Junction	Coupled System
1	0.0001643	0.0001875	0.0	0.0
2	0.0015925	0.0026855	0.0	0.0
3	0.0028042	0.0041093	0.0	0.0
4	0.0060125	0.0092633	0.0182248	0.0004391
5	0.0106416	0.0150311	0.0340668	0.0018329
6	0.0155182	0.0216375	0.0427441	0.0030508
7	0.0191977	0.0226482	——	0.0041589
8	0.0205732	0.0338265	——	0.0068585
9	0.0272657	0.0403184	——	0.0098770
10	0.0350689	0.0459002	——	0.0113959

Table 2. Frequencies of Substructures, Junction, and System - Two-Component Benfield Truss

	Junction Modes in MPF		
	n = 4	n = 5	n = 6
$\frac{(\omega_6)_o^2}{\delta_n^2 - (\omega_6)_o^2}$	0.2268	0.1098	0.0856
$\bar{Q}_{io}^T M_{ij} \psi_n$	0.7121	5.8×10^{-14}	0.1450
$P_n \equiv \frac{\Delta_n (\omega_6)^2}{(\omega_6)_o^2}$	-0.1150	-3.7×10^{-28}	-1.8×10^{-3}

Table 3. Modal Participation Factor Data for Mode 6 (Elastic Mode 3) of Benfield Truss - Base Solution: $N_j = 3$, $N_A = N_B = 5$; $(\omega_6)_o^2 = 0.0033692$; $(\omega_6)_{exact}^2 = 0.0030508$

Elastic Mode Number	$N_j = 6, N_A = N_B = 5$		$N_j = 5, N_A = N_B = 5$		$N_j = 4, N_A = N_B = 5$		$N_j = 3, N_A = N_B = 5$		Exact
	ω^2	% error	ω^2	% error	ω^2	% error	ω^2	% error	
1	0.0004391	0.00	0.0004393	0.05	0.0004393	0.05	0.0004395	0.09	0.0004391
2	0.0018331	0.01	0.0018503	0.95	0.0018506	0.97	0.0018704	2.05	0.0018329
3	0.0030527	0.06	0.0030563	0.18	0.0033691	10.43	0.0033692	10.44	0.0030508
4	0.0041664	0.18	0.0041863	0.66	0.0041864	0.66	0.0042104	1.24	0.0041589
5	0.0068734	0.22	0.0068790	0.30	0.0068790	0.30	0.0068858	0.40	0.0068585
6	0.0098938	0.17	0.0099457	0.70	0.0099459	0.70	0.0100140	1.39	0.0098770
7	0.0126051	10.61	0.0126245	10.78	0.0126245	10.78	0.0126522	11.02	0.0113959
8	0.0144412	18.02	0.0144450	18.05	0.0144474	18.07	0.0144500	18.09	0.0122362
9	0.0161327	7.05	0.0162019	7.51	0.0162019	7.51	0.0163082	8.22	0.0150701
10	0.0246411	58.82	0.0249711	60.95	0.0249735	60.97	0.0257599	66.04	0.0155146
11	0.0361008	x	0.0394011	x	0.0627690	x	---	---	0.0174052
12	0.0506162	x	0.0678697	x	---	---	---	---	0.0200979

Table 4. Frequencies of 2-Component Benfield Truss with Guyan Interface Reductions

due to omission of junction mode 4 from the base solution is 11.50%; the actual error was 10.44% (see Table 1).

The Benfield truss was also used to illustrate the Guyan reduction method. The numbering of the six junction coordinates is shown on Fig. 3. The solution obtained by retaining coordinates 1, 2, and 3 is the same as the $N_j = 3$ solution by the modal reduction method, since this case consists of modelling the interface as a rigid-body. Guyan reduction was employed by first reducing out coordinate 6 (leaving $N_j = 5$), and then reducing out both 5 and 6 ($N_j = 4$). Had other choices been made of coordinates to reduce out, the results would probably have been different from those shown in Table 4.

The results of Tables 1 and 4 are summarized in Fig. 4, which shows a comparison of the number of modes having an accuracy of 0.5% or better. Although modal reduction of interface coordinates yielded slightly better results than Guyan reduction, the present example is too small for any general conclusions to be drawn from it.

Grid examples - modal reduction of substructure normal mode coordinates and junction coordinates. - Figure 5 shows a cantilever grid structure used to illustrate further the modal reduction of junction coordinates. A total of 12 junction coordinates couple the two substructures together.

This grid structure was used to provide an example having more junction coordinates than the truss previously discussed and having no rigid-body freedoms. Studies were made to compare the effect of reducing junction mode coordinates with the effect of reducing substructure normal mode coordinates.

Table 5 gives the frequencies obtained using various combinations of substructure normal modes and junction modes. In all cases, the modes to be retained were selected on the basis of frequency alone. Figure 6 shows a comparison of the number of modes having an accuracy of 0.5% or better. Figure 6 seems to indicate that modal reduction of junction coordinates and reduction of substructure normal mode coordinates produce similar decreases in the number of modes accurate to within 0.5%. Again, the example problem is too small to permit generalizations concerning the effect of modal reduction of junction coordinates, but the results shown in Fig. 6 suggest that, within limits, modal reduction of junction coordinates is feasible.

Since there are only 4 translational coordinates along the junction, it might appear that 4 junction mode coordinates would be adequate to represent junction behavior in a good many, if not all, modes. Case 3 (N_A = 12, N_B = 8, N_j = 4) indicates that this is not so. Note that Mode 9 has a large frequency error (12.03%) in Case 3 but only 0.3 % error in Case 2. It was discovered that the 5th junction mode, i.e., the last one eliminated in going from Case 2 (N_j = 8) to Case 3 (N_j = 4) is predominantly torsion of the junction line, and that this mode contributes significantly to both 9th and 10th system elastic modes.

The above discussion serves to caution against reducing out junction modes using a frequency criterion alone. Modal participation factors, as previously described, should, if possible, be used in choosing which modes to retain. Also, whereas previous studies of Guyan reduction of system coordinates have indicated that most, if not all, rotation coordinates could be reduced out, it is clear from the present example that junction modes in

	EXACT 72 d.o.f.	Case 1 $N_A = 12$, $N_B = 8$ $N_j = 12$		Case 2 $N_A = 12$, $N_B = 8$ $N_j = 8$		Case 3 $N_A = 12$, $N_B = 8$ $N_j = 4$	
	$\omega^2 \times 10^8$	$\omega^2 \times 10^8$	% error	$\omega^2 \times 10^8$	% error	$\omega^2 \times 10^8$	% error
1	.00006210	.00006210	0.00	.00006210	0.00	.00006210	0.00
2	.00025109	.00025109	0.00	.00025109	0.00	.00025109	0.00
3	.00163979	.00163989	0.00	.00164196	0.13	.00164338	0.21
4	.00238797	.00238814	0.00	.00238868	0.03	.00238914	0.05
5	.00394372	.00394381	0.00	.00394410	0.01	.00394562	0.05
6	.00819127	.00819336	0.02	.00819782	0.08	.00820075	0.12
7	.00862821	.00863058	0.02	.00867480	0.54	.00881666	2.18
8	.01806006	.01806936	0.05	.01808240	0.12	.02002345	10.87
9	.01991494	.01992609	0.05	.01999119	0.38	.02231127	12.03
10	.02254916	.02255262	0.01	.02255666	0.03	.02739305	21.48
11	.02744331	.02746586	0.08	.02746796	0.09	.02884310	5.10
12	.03262871	.03265385	0.07	.03281643	0.58	.04300392	31.80
13	.04493968	.04498599	0.10	.04501865	0.18	.05081456	13.07
14	.05150864	.05157714	0.13	.05188925	0.74	.06694802	29.97
15	.06174304	.06186679	0.18	.06199213	0.40	.06874477	11.34
16	.06664190	.06694378	0.45	.06695656	0.47	.07799772	17.04
17	.06963443	.06967930	0.06	.06970706	0.10	.08176796	17.43
18	.08534059	.08547908	0.16	.08552822	0.22	.09683511	13.47
19	.08680764	.08694733	0.16	.08802157	1.40	.10838887	24.86
20	.08914933	.08962024	0.52	.08985521	0.79	.12193065	36.77
21	.11610254	.11642648	0.28	.11674719	0.56	.17152633	47.74
22	.13869278	.13978448	0.79	.14089915	1.60	.19322336	39.32
23	.16186275	.16221708	0.22	.16348153	1.00	.68624299	
24	.22210384	.22437005	1.02	.22687256	2.15	.83847870	
25	.37412949	.54848664		.68470672		---	
26	.42607786	.68464932		.81364585		---	
27	.45121738	.81363654		.99749775		---	
28	.45215748	.99798215		1.19928682		---	
29	.50738107	1.11532496		---		---	
30	.55621118	1.20968364		---		---	
31	.57430761	2.64433441		---		---	
32	.61043891	5.77733431		---		---	

Table 5. Frequencies of Cantilever Grid Structure

	Case 4		Case 5		Case 6	
	$N_A = 10$, $N_B = 6$ $N_j = 12$		$N_A = 7$, $N_B = 5$ $N_j = 12$		$N_A = 5$, $N_B = 3$ $N_j = 12$	
	$\omega^2 \times 10^8$	% error	$\omega^2 \times 10^8$	% error	$\omega^2 \times 10^8$	% error
1	.00006210	0.00	.00006210	0.00	.00006211	0.01
2	.00025109	0.00	.00025109	0.00	.00025115	0.02
3	.00163996	0.01	.00164019	0.02	.00164660	0.41
4	.00238879	0.03	.00239012	0.09	.00239788	0.41
5	.00394429	0.01	.00394433	0.01	.00395306	0.23
6	.00819481	0.04	.00819496	0.04	.00871273	6.36
7	.00863617	0.09	.00867873	0.58	.00881859	2.20
8	.01822469	0.91	.01825831	1.09	.01857390	2.84
9	.01995132	0.18	.01997539	0.30	.02188961	9.91
10	.02267161	0.54	.02267290	0.54	.02271096	0.71
11	.02748344	0.14	.02750874	0.23	.03865739	40.82
12	.03313560	1.55	.03320131	1.75	.06218932	x
13	.04505185	0.24	.05276010	17.40	.08120924	x
14	.05672962	10.14	.05686502	10.39	.12613476	x
15	.06272867	1.58	.06696988	8.44	.20728453	x
16	.06695281	0.46	.08138276	22.11	.36264343	x
17	.07023630	0.86	.27636744	x	.53033012	x
18	.08792538	3.02	.35125316	x	1.05181024	x
19	.08987727	3.53	.39979778	x	2.45246230	x
20	.12568251	40.97	.53601805	x	5.23913299	x
21	.29256023	x	.70526557	x	---	
22	.54288243	x	1.07483996	x	---	
23	.61782701	x	2.55507900	x	---	
24	.70712486	x	5.43404880	x	---	
25	.83876447	x	---		---	
26	1.10079821	x	---		---	
27	2.59004208	x	---		---	
28	5.58769127	x	---		---	
29	---		---		---	
30	---		---		---	
31	---		---		---	
32	---		---		---	

Table 5 (cont.). Frequencies of Cantilever Grid Structure

which "twist" of the junction line is significant may be important to the accuracy of system frequencies obtained through the use of modal reduction of junction coordinates.

Ring examples - Ritz reduction of junction coordinates. - Figure 7 shows a ring structure which was used to provide examples of Ritz reduction of junction coordinates. The ring was divided into nine substructures, with each substructure having eight elements. Since each element subtends an arc of only five degrees, a straight beam element was used, with the translational coordinates transformed to the radial and circumferential orientation at the nodes. Although they participated very little in the solution for the first ten system modes, two substructure normal modes were included for each substructure in generating the substructure coordinates q_i in Eq. (17).

Two cases are presented: (1) a uniform ring, which possesses symmetry properties and for which an analytical solution is available, and (2) a non-axisymmetric stiffened ring. In each case solutions employing a Ritz approximation of junction coordinates based on Eqs. (63) and (67) are compared with solutions employing all 27 junction coordinates plus 18 substructure normal modes, as noted above.

For the Ritz approximation using 15 Ritz vectors, the junction displacements were assumed to have the form

$$\bar{v}_i = \begin{bmatrix} 1 & \cos(\beta_i) & \sin(\beta_i) & \cos(2\beta_i) & \sin(2\beta_i) \end{bmatrix} \begin{Bmatrix} v_1 \\ v_2 \\ v_3 \\ v_4 \\ v_5 \end{Bmatrix} \tag{82}$$

and similarly for $\bar{w}_i$ and $\bar{\theta}_i$. Thus, the number of junction coordinates was reduced from 27 to 15. In this problem the junction coordinates are far more important than the substructure normal mode coordinates, and it would have been better to retain all 27 junction coordinates and to delete all substructure modal coordinates. However, the present example should serve to emphasize that reduction of junction coordinates, by any strategy, requires careful consideration of the particular problem at hand.

For the uniform ring an analytical solution is available (ref. 12). There are three rigid-body modes. These may be given by:

Mode 1: $\bar{\theta}_i = 0, \quad \bar{w}_i = \cos \beta_i, \quad \bar{v}_i = -\sin \beta_i$

Mode 2: $\bar{\theta}_i = 0, \quad \bar{w}_i = \sin \beta_i, \quad \bar{v}_i = \cos \beta_i$

Mode 3: $\bar{w}_i = 0, \quad \bar{v}_i = 1, \quad \bar{\theta}_i = -1/R$

The first two are translation modes; the third represents rotation about the axis of the ring. Of course, any linear combination of the above rigid-body modes is also a rigid-body mode.

The elastic in-plane bending modes can be expressed in terms of a trigonometric series in β_i. A simple solution is obtained if it is assumed that,

for flexural vibration, the ring is inextensional (ref. 12). In this case, the eigenvalues of the ring are given by

$$\omega_n^2 = \frac{EI\, n^2(1 - n^2)^2}{\rho\, AR^4(1 + n^2)} \tag{83}$$

where n = 2 corresponds to the lowest flexural elastic mode.

Table 6 gives the frequencies obtained for the uniform ring. The solutions based on Eq. (23) and on Eq. (67) are compared with the analytical solution given in Eq. (83).

Method / Elastic Mode	All 27 Junction Coordinates Eq. (23)	15 Ritz Junction Coordinates Eq. (67)	Analytical Eq. (83)
1	2.6558×10^3	2.6558×10^3	2.6541×10^3
2	2.6558×10^3	2.6558×10^3	2.6541×10^3
3	2.1249×10^4	8.3493×10^5	2.1233×10^4
4	2.1249×10^4	8.3493×10^5	2.1233×10^4
5	7.8145×10^4	1.4456×10^6	7.8061×10^4
6	7.8145×10^4	1.4456×10^6	7.8061×10^4
7	2.0450×10^5	2.3357×10^6	2.0416×10^5

Table 6. Eigenvalues (ω^2) of a Uniform Ring

From Table 6 it can be seen that the coupled system solution that includes all 27 junction coordinates produces accurate frequencies, while only the first two elastic mode frequencies are computed accurately by the Ritz representation of junction coordinates. This occurs, of course, since the exact mode shapes of higher-frequency modes are orthogonal to the Ritz vectors included in Eq. (82). As would be expected, the mode shapes of elastic modes 1 and 2 of the Ritz solution are composed almost entirely of $\cos(2\beta_j)$ and sin $\sin(2\beta_j)$ terms. Other terms are negligible in these modes.

Table 7 gives the frequencies of the non-symmetric ring. A solution of Eq. (23) containing all 27 junction coordinates is compared with results obtained using the Ritz approximation of Eq. (67) with 15 Ritz vectors (as in Eq. (82)) and 21 Ritz vectors. The latter solution included $\cos(3\beta_j)$ and $\sin(3\beta_j)$ terms for $\bar{v}_j$, $\bar{w}_j$, and $\bar{\theta}_j$.

Note first, from Table 7, that the coupled solution in column one reflects a slight raising of frequencies due to the stiffening of the ring and that the frequencies no longer occur in pairs. Secondly, note that neither of the Ritz approximations of junction coordinates is any good even though, in column three, the number of Ritz coordinates is almost 80% of the total number of physical junction coordinates. Perhaps for the ring it would be possible to choose more "efficient" Ritz vectors than those represented in Eq. (82). However, it can be argued that these are certainly logical for the present problem.

Method Elastic Mode	All 27 Junction Coordinates Eq. (23)	15 Ritz Vectors Eq. (67)	21 Ritz Vectors Eq. (67)
1	3.3127×10^3	5.6348×10^3	4.1139×10^3
2	3.8962×10^3	6.0030×10^3	5.4910×10^3
3	2.8204×10^4	1.2210×10^6	3.7653×10^4
4	3.4333×10^4	1.2488×10^6	4.1730×10^4
5	1.0854×10^5	2.2502×10^6	6.1599×10^5
6	1.2269×10^5	2.2889×10^6	6.9169×10^5
7	2.8513×10^5	3.5847×10^6	1.2342×10^6

Table 7. Eigenvalues (ω^2) of Non-axisymmetric Ring

Equation (81) was applied to determine whether the addition of a $\cos(3\beta_i)$ contribution to the radial displacements, $\bar{w}_i$, would produce a significant change in the frequency of the third elastic mode considering the solution with 15 Ritz vectors to be the base problem. A value of $(\Delta\omega^2/\omega_o^2)$ of order 10^4 was obtained, indicating that this contribution would be very significant. A numerical value this high obviously violates any "small perturbation" assumption on $\Delta\omega^2/\omega_o^2$, but it does signify that the base problem solution for this mode would be too inaccurate to be useful. As a matter of fact, the solution

based on 21 Ritz vectors shows the $\cos(3\beta_i)$ and $\sin(3\beta_i)$ contributions to $\bar{v}_i$, $\bar{w}_i$, and $\bar{\theta}_i$ to be dominant in the third elastic mode.

IMPROVEMENT OF FREE-INTERFACE METHODS

In this part of the report attention is directed toward ways of improving the accuracy of free-interface methods. Example problems are solved and the results are compared with those of a fixed-interface method and a commonly used free-interface method.

Substructure Equations

As in Eq. (3) the substructure equation of motion may be written in partitioned form as

$$\begin{bmatrix} m_{ii} & m_{ij} \\ m_{ji} & m_{jj} \end{bmatrix} \begin{Bmatrix} \ddot{x}_i \\ \ddot{x}_j \end{Bmatrix} + \begin{bmatrix} k_{ii} & k_{ij} \\ k_{ji} & k_{jj} \end{bmatrix} \begin{Bmatrix} x_i \\ x_j \end{Bmatrix} = \begin{Bmatrix} 0 \\ f_j \end{Bmatrix} \tag{84}$$

The free-interface modes of the substructure are obtained by setting $f_j = 0$ in Eq. (84) and solving the resulting equation

$$m\ddot{x} + kx = 0 \tag{85}$$

The modes, ϕ_n, may be normalized so that

$$\phi_n^T m \phi_n = 1 \tag{86}$$

$$\phi_n^T k \phi_n = \lambda_n^2 \tag{87}$$

The modes are assembled to form the modal matrix, Φ, which defines substructure generalized coordinates through the equation

$$x = \Phi p \tag{88}$$

The modal matrix may be partitioned as follows:

$$\Phi = \begin{bmatrix} \Phi_{ik} & \Phi_{ia} \\ \Phi_{jk} & \Phi_{ja} \end{bmatrix} \tag{89}$$

where "k" stands for kept and "a" stands for approximated. That is, the full modal information of the "k" modes will be kept, but the "a" modes will be approximated.

When Eq. (88) is substituted into Eq. (84), there results a set of uncoupled equations of the form

$$\ddot{p}_n + \lambda_n^2 p_n = g_n(t) \tag{90}$$

where

$$g_n(t) = \phi_{jn}^T f_j \tag{91}$$

where ϕ_{jn} is the partition of the nth substructure mode associated with junction coordinates (since, for free vibration the only external forcing of a substructure is through its interface).

Consider now harmonic motion, as would be present in free vibration. Let a bar over a symbol indicate the magnitude, e.g.,

$$p_n(t) = \bar{p}_n \cos(\omega t) \tag{92}$$

Equations (90) and (92) lead to

$$\bar{p}_n = \frac{\bar{g}_n}{\lambda_n^2 - \omega^2} \tag{93}$$

The physical displacements under harmonic motion can be obtained by combining Eqs. (88) and (93) to obtain

$$\bar{x} = \sum_{n=1}^{N} \left(\frac{\bar{g}_n}{\lambda_n^2 - \omega^2} \right) \phi_n \tag{94}$$

where ϕ_n is the nth mode shape and N is the total number of modes of the substructure.

Equation (94) may be written in a form which suggests the basis for the approximation methods of MacNeal (ref. 7) and Rubin (ref. 6), namely

$$\bar{x} = \sum_{n=1}^{S} \left(\frac{\bar{g}_n}{\lambda_n^2 - \omega^2} \right) \phi_n + \sum_{n=S+1}^{N} \left(\frac{\bar{g}_n}{\lambda_n^2 - \omega^2} \right) \phi_n \tag{95}$$

If the second series in Eq. (95) corresponds to modes for which $\lambda_n >> \omega$, this series may be approximated by the static effects only, and Eq. (95) becomes

$$\bar{x} = \sum_{n=1}^{S} \left(\frac{\bar{g}_n}{\lambda_n^2 - \omega^2} \right) \phi_n + \sum_{n=S+1}^{N} \left(\frac{\bar{g}_n}{\lambda_n^2} \right) \phi_n \tag{96}$$

This corresponds to the concept of "residual flexibility" discussed by Klosterman (ref. 8). The point stressed by Rubin (ref. 6) is that the modes and frequencies indicated in the second series of Eq. (96) do not need to be obtained explicitly. This will be explained in the following paragraphs. The discussion will be restricted to harmonic motion of undamped structures since this is the situation encountered in the determination of modes and frequencies of a system.

If the "dynamics" were neglected in Eq. (84), a "pseudo-static response," x_f, could be obtained by solving the equation

$$k\, x_f = f \tag{97}$$

If the substructure has rigid-body freedom, k will be singular and the solution of Eq. (97) for x_f requires special consideration of this fact. Thus, the first and second-order approximation methods will be described first for constrained substructures, for which k is non-singular, and then the approximation methods will be developed for free substructures.

Constrained substructures - first-order method. - For harmonic forcing, $f = \bar{f} \cos(\omega t)$, Eq. (97) gives

$$k\, \bar{x}_f^{(1)} = \bar{f} \tag{98}$$

or

$$\bar{x}_f^{(1)} = G\, \bar{f} \tag{99}$$

where G is the flexibility matrix and the superscript (1) identifies this as the first-order response. Since, for free vibration of a substructure,

external forces act only at junction coordinates, only the columns of G associated with junction coordinates are required.

In Eq. (96) the second series represents the pseudo-static response of the higher-frequency modes ($n \geq S + 1$), whereas $\bar{x}_f^{(1)}$ in Eq. (99) contains contributions from all modes. It is assumed that the modes to be kept, together with their natural frequencies, are available. Let Eq. (89) be written

$$\Phi = [\, \Phi_k \; \Phi_a \,] \tag{100}$$

then the pseudo-static response, based on Eq. (88) is

$$\bar{x}_f^{(1)} = \Phi_k \, d_k^{(1)} + \Phi_a \, d_a^{(1)} \tag{101}$$

or

$$\bar{x}_f^{(1)} = \bar{x}_k^{(1)} + \bar{x}_a^{(1)} \tag{102}$$

where

$$\bar{x}_k^{(1)} = \Phi_k \, d_k^{(1)} \tag{103}$$

and

$$\bar{x}_a^{(1)} = \Phi_a \, d_a^{(1)} \tag{104}$$

Since the modes in Φ_a are not, in general, available, it is necessary to use Eqs. (99) and (102) to obtain $\bar{x}_a^{(1)}$. To that end, let Eq. (101) be substituted into Eq. (98) and let the resulting equation be premultiplied by Φ^T, giving

$$\begin{bmatrix} \Phi_k^T \\ \Phi_a^T \end{bmatrix} [k] [\Phi_k \ \Phi_a] \begin{Bmatrix} d_k^{(1)} \\ d_a^{(1)} \end{Bmatrix} = \begin{bmatrix} \Phi_k^T \\ \Phi_a^T \end{bmatrix} \{ \bar{f} \} \tag{105}$$

Since all of the modes are mutually orthogonal with respect to k,

$$\Phi_k^T \, k \, \Phi_a = \Phi_a^T \, k \, \Phi_k = 0 \tag{106}$$

Also, from Eq. (87)

$$\Phi_k^T \, k \, \Phi_k = \Lambda_k \tag{107}$$

and

$$\Phi_a^T \, k \, \Phi_a = \Lambda_a \tag{108}$$

where Λ_k and Λ_a are diagonal matrices composed of the respective values of λ_n^2 . Thus, from Eq. (105) is obtained a set of uncoupled equations expressed collectively by

$$\Lambda_k \, d_k^{(1)} = \Phi_k^T \, \bar{f} \tag{109}$$

Thus,

$$d_k^{(1)} = \Lambda_k^{-1} \, \Phi_k^T \, \bar{f} \tag{110}$$

Equations (103) and (110) may be combined to give

$$\bar{x}_k^{(1)} = G_k^{(1)} \, \bar{f} \tag{111}$$

where

$$G_k^{(1)} = \Phi_k \Lambda_k^{-1} \Phi_k^T \tag{112}$$

From Eqs. (99), (102), and (111) is obtained an expression for the contribution of the approximated modes to the pseudo-static response, namely

$$\bar{x}_a^{(1)} = G_a^{(1)} \bar{f} \tag{113}$$

where

$$G_a^{(1)} = G - G_k^{(1)} \tag{114}$$

Equation (113) expresses what Rubin calls the first-order contribution of the residual, or approximated, modes.

The first-order method, which will also be referred to as the MacNeal method, may be summarized by the following equations:

$$(-\omega^2 I + \Lambda_k) \bar{p}_k = \Phi_{jk}^T \bar{f}_j \tag{115}$$

which is obtained from Eq. (90) for harmonic motion. Equation (96) may be written in matrix form as

$$\bar{x}^{(1)} = \Phi_k \bar{p}_k + G_a^{(1)} \bar{f} \tag{116}$$

This equation will be needed when substructures are coupled to form the complete structure. In that case, the physical displacements of junction coordinates are required. These are given by the appropriate partition of Eq. (116), namely

$$\bar{x}_j^{(1)} = \Phi_{jk}\, \bar{p}_k + G_{jj}^{(1)}\, \bar{f}_j \tag{117}$$

where $G_{jj}^{(1)}$ is taken from the appropriate rows and columns of $G_a^{(1)}$. Thus, Eqs. (115) and (117) are the relevant substructure equations.

Constrained substructures - second-order method. - For harmonic motion, Eq. (84) can be written

$$k\,\bar{x} = \bar{f} + \omega^2\, m\,\bar{x} \tag{118}$$

Rubin (ref. 6) obtains the second approximation by putting the pseudo-static first approximation, $\bar{x}_f^{(1)}$, on the right had side of Eq. (118) and solving for the $\bar{x}$ on the left hand side. Thus, the pseudo-static second approximation is given by

$$\bar{x}_f^{(2)} = G(\bar{f} + \omega^2\, m\, \bar{x}_f^{(1)}) \tag{119}$$

As in Eqs. (101) and (102)

$$\bar{x}_f^{(2)} = \Phi_k\, d_k^{(2)} + \Phi_a\, d_a^{(2)} \tag{120}$$

or

$$\bar{x}_f^{(2)} = \bar{x}_k^{(2)} + \bar{x}_a^{(2)} \tag{121}$$

Equations (99) and (119) can be combined to give

$$\bar{x}_f^{(2)} = G\,(I + \omega^2\, m\, G)\,\bar{f} \tag{122}$$

By analogy with the previous derivation of Eq. (111)

$$\bar{x}_k^{(2)} = G_k^{(1)}\,(\bar{f} + \omega^2\, m\, \bar{x}_f^{(1)}) \tag{123}$$

or

$$\bar{x}_k^{(2)} = G_k^{(1)} (I + \omega^2 m G) \bar{f} \tag{123}$$

Thus, the second-order approximation of the residual (approximated) modes is given by

$$\bar{x}_a^{(2)} = \bar{x}_f^{(2)} - \bar{x}_k^{(2)} \tag{124}$$

or

$$\bar{x}_a^{(2)} = G_a^{(2)} \bar{f} \tag{125}$$

where

$$G_a^{(2)} = (G - G_k^{(1)}) (I + \omega^2 m G) \tag{126}$$

This can be simplified as follows:

$$(G - G_k^{(1)}) (I + \omega^2 m G) =$$

$$G_a^{(1)} [I + \omega^2 m (G_a^{(1)} + G_k^{(1)})] =$$

$$G_a^{(1)} + \omega^2 G_a^{(1)} m G_a^{(1)} + \omega^2 G_a^{(1)} m G_k^{(1)}$$

But,

$$G_a^{(1)} m G_k^{(1)} = \Phi_a \Lambda_a^{-1} \Phi_a^T m \Phi_k \Lambda_k^{-1} \Phi_k^T$$

from Eq. (112). Due to orthogonality, the above vanishes. Hence,

$$G_a^{(2)} = G_a^{(1)} (I + \omega^2 m G_a^{(1)}) \tag{127}$$

or

$$G_a^{(2)} = G_a^{(1)} + \omega^2 H_a^{(1)} \tag{128}$$

where

$$H_a^{(1)} = G_a^{(1)} m G_a^{(1)} \tag{129}$$

The second-order approximation may be summarized by the following equations:

$$(- \omega^2 I + \Lambda_k) \bar{p}_k = \Phi_{jh}^T \bar{f}_j \tag{130}$$

which is the same as Eq. (115), is the primary equation for determining $\bar{p}_k$ To effect coupling, the physical displacement equation is required, namely

$$\bar{x}^{(2)} = \Phi_k \bar{p}_k + G_a^{(2)} \bar{f} \tag{131}$$

The corresponding junction point displacements are given by

$$\bar{x}^{(2)} = \Phi_{jk} \bar{p}_k + G_{jj}^{(2)} \bar{f}_j \tag{132}$$

where $G_{jj}^{(2)}$ is the appropriate partition of $G_a^{(2)}$.

Unconstrained substructures. - If a substructure possesses one or more rigid-body degrees of freedom it will be referred to as an unconstrained substructure. Since k is singular, the flexibility matrix, G, used in the preceding analysis does not exist. On the other hand, since aerospace structures by nature possess rigid-body freedom, it is important that methods be developed to analyze such structures by substructure methods similar to the

foregoing ones. Rubin's paper (ref. 6) was devoted to this case.

For a substructure possessing rigid-body freedom, let the displacement be given by

$$x = x_r + x_f \tag{133}$$

where x_r is rigid-body motion and x_f is (relative) flexible motion. Also, let the modes of the structure be separated into rigid-body and flexible modes such that

$$x = \Phi_r p_r + \Phi_f p_f \tag{134}$$

In the notation of preceding sections all of the rigid-body modes, i.e., Φ_r, would be kept as would a limited number of flexible-body modes. The remaining flexible-body modes would be approximated. Since x_f cannot be obtained by inverting k, as was done in going from Eq. (98) to Eq. (99), it is necessary to "remove" the rigid-body motion.

Let Eq. (134) be substituted into Eq. (84) and the resulting equation be pre-multiplied by Φ^T to give the uncoupled equations

$$\ddot{p}_r = \Phi_r^T f \tag{135}$$

and

$$\ddot{p}_f + \Lambda_f p_f = \Phi_f^T f \tag{136}$$

where the orthogonality of modes is employed and it is assumed that modes are normalized so that

$$\Phi_r^T m \Phi_r = I \tag{137}$$

and

$$\Phi_f^T m \Phi_f = I \tag{138}$$

From Eq. (135) it is seen that, as far as rigid-body motion is concerned, the external forces are reacted by rigid-body inertia forces. Hence, if these rigid-body inertia forces are subtracted from the applied force, f, there will be no excitation of rigid-body modes. The physical displacement due to rigid-body modes is

$$x_r = \Phi_r p_r \tag{139}$$

so the (reversed) inertia force vector is given by

$$f_i = - m \ddot{x}_r = - m \Phi_r \Phi_r^T f \tag{140}$$

Thus, the net force producing flexible-body motion is given by

$$f_f = f + f_i = A f \tag{141}$$

where

$$A = I - m \Phi_r \Phi_r^T \tag{142}$$

To determine the flexible-body motion resulting from f_f it is necessary to impose temporary constraints on the substructure so that rigid-body motion is prevented. Let G_c be the flexibility matrix of the structure which has been subjected to arbitrary statically-determinate constraints. G_c may be obtained by taking k (which is singular), deleting rows and columns corresponding to the constrained degrees of freedom, inverting to get a flexibility matrix, and expanding the flexibility matrix by inserting zeros in rows and

columns corresponding to the constraints. The resulting augmented flexibility matrix is called G_c.

The flexible-body displacement relative to the imposed constraints is given by

$$\begin{aligned} x_c^{(1)} &= G_c\,(f + f_i) \\ &= G_c\,A\,f \end{aligned} \tag{143}$$

To obtain the flexible-body displacement, $x_f^{(1)}$, rigid-body motion is removed from $x_c^{(1)}$ by making $x_f^{(1)}$ orthogonal to all rigid-body modes, i.e.,

$$\Phi_r^T\, m\, x_f^{(1)} = 0 \tag{144}$$

where

$$x_f^{(1)} = x_c^{(1)} + \Phi_r\, c_r \tag{145}$$

Thus,

$$x_f^{(1)} = x_c^{(1)} - \Phi_r\, \Phi_r^T\, m\, x_c^{(1)} \tag{146}$$

or

$$x_f^{(1)} = A^T\, x_c^{(1)} \tag{147}$$

From Eqs. (143) and (147)

$$x_f^{(1)} = (A^T\, G_c\, A)\, f \tag{148}$$

Equation (148) and Eq. (99) serve the same purpose for free substructures and constrained substructures respectively. Thus, let the symbol G be defined, for free substructures, by

$$G = A^T G_c A \tag{149}$$

With this definition of G for free substructures, the remainder of the derivation of first and second-order methods proceeds as before, beginning with Eq. (99).

Coupling of Substructures

In the preceding sections the substructure equations have been obtained for both constrained and free substructures. In the present section equations will be developed for coupling substructures. Figure 8 shows two substructures, together with the junction coordinates at which compatibility must be enforced. Since there are differences in the substructure equations of the first-order and second-order methods, these will be treated separately.

Coupling for the first-order approximation. - Equations (115) and (117) are the pertinent substructure equations for the first-order approximation. For substructure A they can be written

$$\bar{x}^{(1)}_{jA} = \Phi_{jkA}\, \bar{p}_{kA} + G^{(1)}_{jjA}\, \bar{f}_{jA} \tag{150}$$

and

$$(- \omega^2 I + \Lambda_{kA})\, \bar{p}_{kA} = \Phi^T_{jkA}\, \bar{f}_{jA} \tag{151}$$

For substructure B

$$\bar{x}^{(1)}_{jB} = \Phi_{jkB}\, \bar{p}_{kB} + G^{(1)}_{jjB}\, \bar{f}_{jB} \tag{152}$$

and

$$(- \omega^2 I + \Lambda_{kB}) \bar{p}_{kB} = \Phi^T_{jkB} \bar{f}_{jB} \tag{153}$$

The junction coordinates of A and B must coincide. However, the number of "kept" modes of A and "kept" modes of B may be different.

The coupling equations are

$$\bar{x}_{jA} = \bar{x}_{jB} \tag{154}$$

and

$$\bar{f}_{jA} = - \bar{f}_{jB} \tag{155}$$

where it is assumed that any required coordinate transformations have been made so that the junction coordinates of A coincide with the junction coordinates of B as given by the compatibility equation, Eq. (154). Equations (150), (152) and (155) may be substituted into Eq. (154) to give

$$\bar{f}_{jA} = (G^{(1)}_{jjA} + G^{(1)}_{jjB})^{-1} (\Phi_{jkB} \bar{p}_{kB} - \Phi_{jkA} \bar{p}_{kA}) \tag{156}$$

Equation (156) may now be substituted into Eq. (151) to give

$$(- \omega^2 I + \Lambda_{kA}) \bar{p}_{kA} = \Phi^T_{jkA} (G^{(1)}_{jjA} + G^{(1)}_{jjB})^{-1} (\Phi_{jkB} \bar{p}_{kB} - \Phi_{jkA} \bar{p}_{kA}) \tag{157}$$

Similarly, Eqs. (155) and (156) may be substituted into Eq. (153) to give

$$(- \omega^2 I + \Lambda_{kB}) \bar{p}_{kB} = - \Phi^T_{jkB} (G^{(1)}_{jjA} + G^{(1)}_{jjB})^{-1} (\Phi_{jkB} \bar{p}_{kB} - \Phi_{jkA} \bar{p}_{kA}) \tag{158}$$

Equations (157) and (158) may then be combined to form the equation

$$\begin{bmatrix} K_{AA} & K_{AB} \\ K_{BA} & K_{BB} \end{bmatrix} \begin{Bmatrix} \bar{p}_{kA} \\ \bar{p}_{kB} \end{Bmatrix} = \omega^2 \begin{Bmatrix} \bar{p}_{kA} \\ \bar{p}_{kB} \end{Bmatrix} \tag{159}$$

where

$$\begin{aligned} K_{AA} &= \Lambda_{kA} + \Phi_{jkA}^T \, k^{(1)} \, \Phi_{jkA} \\ K_{AB} &= - \Phi_{jkA}^T \, k^{(1)} \, \Phi_{jkB} \\ K_{BA} &= - \Phi_{jkB}^T \, k^{(1)} \, \Phi_{jkA} \\ K_{BB} &= \Lambda_{kB} + \Phi_{jkB}^T \, k^{(1)} \, \Phi_{jkB} \end{aligned} \tag{160}$$

where

$$k^{(1)} = \left(G^{(1)}_{jjA} + G^{(1)}_{jjB} \right)^{-1} \tag{161}$$

Equation (159) thus forms the primary eigenvalue problem for determining the modes and frequencies of the coupled structure. It may be noted that its size is equal to the sum of the kept substructure modes in substructures A and B.

Coupling for the second-order approximation. - The coupling equations for the second-order approximation can be obtained from Eqs. (157) and (158) by replacing $G^{(1)}_{jj}$ by $G^{(2)}_{jj}$ for the substructure. The complication arises due to the fact that $G^{(2)}_{jj}$ is a submatrix of $G^{(2)}_{a}$, which is given by Eq. (128) as

$$G_a^{(2)} = G_a^{(1)} + \omega^2 H_a^{(1)} \tag{128}$$

Thus,

$$G_{jjA}^{(2)} = G_{jjA}^{(1)} + \omega^2 H_{jjA}^{(1)} \tag{162}$$

and

$$G_{jjB}^{(2)} = G_{jjB}^{(1)} + \omega^2 H_{jjB}^{(1)} \tag{163}$$

Let

$$G_{jjA}^{(1)} + G_{jjB}^{(1)} = G_{jj}^{(1)} \tag{164}$$

and

$$H_{jjA}^{(1)} + H_{jjB}^{(1)} = H_{jj}^{(1)} \tag{165}$$

Then,

$$G_{jjA}^{(2)} + G_{jjB}^{(2)} = G_{jj}^{(1)} + \omega^2 H_{jj}^{(1)} \tag{166}$$

From Eqs. (157) and (158) the system equations for the second-order method may be deduced to be

$$\left[\begin{array}{c|c} \Lambda_{kA} + \Phi_{jkA}^T k^{(2)} \Phi_{jkA} & -\Phi_{jkA} k^{(2)} \Phi_{jkB} \\ \hline -\Phi_{jkB}^T k^{(2)} \Phi_{jkA} & \Lambda_{kB} + \Phi_{jkB} k^{(2)} \Phi_{jkB}^T \end{array}\right] \left\{\begin{array}{c} \bar{p}_{kA} \\ \hline \bar{p}_{kB} \end{array}\right\} = \omega^2 \left\{\begin{array}{c} \bar{p}_{kA} \\ \hline \bar{p}_{kB} \end{array}\right\} \tag{167}$$

where

$$k^{(2)} = \left(G^{(2)}_{jjA} + G^{(2)}_{jjB} \right)^{-1} = \left(G^{(1)}_{jj} + \omega^2 H^{(1)}_{jj} \right)^{-1} \qquad (168)$$

Since, from Eqs. (166), ω^2 appears on both the left and right-hand sides of Eq. (167) this system equation cannot be solved conveniently in its present form. Two methods may be used to circumvent this difficulty: (1) an iteration method may be used, with the ω^2 on the left-hand side of Eq. (167) being taken, in the first iteration, as the ω^2 obtained by using the first-order method, or (2) a Maclaurin series expansion may be employed to obtain an approximation to the inverse matrix required on the left-hand side of the system equation.

The Maclaurin series method will be described more fully now. Let

$$\begin{aligned} k^{(2)} &= \left(G^{(1)}_{jj} + \omega^2 H^{(1)}_{jj} \right)^{-1} \\ &= \left(G^{(1)}_{jj} \left[I + \omega^2 \left(G^{(1)}_{jj}\right)^{-1} H^{(1)}_{jj} \right] \right)^{-1} \\ &= \left[I + \omega^2 k^{(1)} H^{(1)}_{jj} \right]^{-1} k^{(1)} \end{aligned} \qquad (169)$$

From Eq. (169) it can be seen that the second term in the square bracket distinguishes the second-order method from the first-order method. If the corrections are "small" $k^{(2)}$ can be approximated by

$$k^{(2)} = \left(I - \omega^2 k^{(1)} H^{(1)}_{jj} \right) k^{(1)} \qquad (170)$$

From Eqs. (167) and (170) the following second-order system equation is obtained

$$\begin{bmatrix} K_{AA} & K_{AB} \\ K_{BA} & K_{BB} \end{bmatrix} \begin{Bmatrix} \bar{p}_{kA} \\ \bar{p}_{kB} \end{Bmatrix} = \omega^2 \begin{bmatrix} M_{AA} & M_{AB} \\ M_{BA} & M_{BB} \end{bmatrix} \begin{Bmatrix} \bar{p}_{kA} \\ \bar{p}_{kB} \end{Bmatrix} \tag{171}$$

where

$$\begin{aligned} M_{AA} &= I + \Phi_{jkA}^T \, m^{(1)} \, \Phi_{jkA} \\ M_{AB} &= - \Phi_{jkA}^T \, m^{(1)} \, \Phi_{jkB} \\ M_{BA} &= - \Phi_{jkB}^T \, m^{(1)} \, \Phi_{jkA} \\ M_{BB} &= I + \Phi_{jkB}^T \, m^{(1)} \, \Phi_{jkB} \end{aligned} \tag{172}$$

where

$$m^{(1)} = k^{(1)} \, H_{jj}^{(1)} \, k^{(1)} \tag{173}$$

Examples

Several example problems were solved by the free-interface methods described in the preceding sections. The purpose of these examples is to illustrate the results obtainable by the first-order and second-order methods and to compare these results with those obtained by using a fixed-interface method (method of Craig and Bampton) and another free-interface method (Hou's method).

Beam examples - first and second-order methods versus Hou method. - Frequencies of a two-substructure uniform beam were obtained for three separate sets of boundary conditions: clamped-clamped, clamped-free, and free-free. Thus, the theory for both constrained and free substructures was employed in these examples. Figure 9 shows the configuration of the two substructures for each of the three support conditions. Substructure A consists of four elements, while substructure B consists of three elements. Consistent mass matrices were employed for element mass matrices.

In Table 8 are shown the system frequencies obtained for the clamped-clamped beam by Hou's method and by the first and second-order methods. To obtain each frequency by the second-order method, the iteration procedure was employed, wherein the corresponding frequency obtained by the first-order method was used in determining the $k^{(2)}$ of Eq. (168).

Note that the first-order (MacNeal) method is much more accurate than Hou's method, and that further improvement is obtained by use of the second-order (Rubin) method. On the other hand, increasing the number of substructure modes while using the first-order method also produces significant

improvement.

The "exact" values in Table 8 were obtained by retaining all original physical coordinates.

Table 9 shows a more limited set of results for the clamped-free beam. The accuracy of the first-order method is not as good as it was for the clamped-clamped beam; but the first-order method is still far superior to Hou's method.

Table 10 gives results obtained for the free-free beam. Note that the results obtained by the first-order method are virtually identical to those obtained for the clamped-clamped beam. Of course, the free-free beam has two zero-frequency rigid-body modes which are not listed in the table. Again Hou's method does not produce acceptable accuracy.

Elastic Mode Number	$N_A = 4$, $N_B = 3$		$N_A = 4$, $N_B = 3$		$N_A = 4$, $N_B = 3$		$N_A = 6$, $N_B = 4$		Exact
	1st Order (MacNeal)	% error	2nd order (Rubin)	% error	Hou	% error	1st order (MacNeal)	% error	
1	.0002086	0.05	.0002085	0.00	.0002483	19.09	.0002085	0.00	.0002085
2	.0015878	0.02	.0015875	0.00	.0017281	8.86	.0015876	0.01	.0015875
3	.0061452	0.14	.0061369	0.00	.0072344	17.89	.0061380	0.02	.0061367
4	.0170708	0.54	.0169846	0.03	.0229454	35.13	.0169977	0.10	.0169799
5	.0389090	0.68	.0386883	0.10	.0419588	8.57	.0386634	0.04	.0386480
6	.0795906	5.24	.0764849	1.14	---	--	.0761386	0.68	.0756248
7	.4027931	x	.1967858	20.39	---	--	.1642528	0.48	.1634623

Table 8. Frequencies of a Two-Substructure Clamped-Clamped Beam

Elastic Mode Number	$N_A = 4$, $N_B = 4$		$N_A = 4$, $N_B = 4$		Exact
	1st order (MacNeal)	% error	Hou	% error	
1	.0000052	0.00	.0000053	1.92	.0000052
2	.0002069	2.27	.0002624	29.71	.0002023
3	.0016227	2.15	.0017612	10.86	.0015886
4	.0061338	0.01	.0072102	17.56	.0061330
5	.0177475	4.73	.0228454	34.81	.0169463
6	.0385308	0.21	.0418527	8.85	.0384504
7	.0828725	10.58	---	--	.0749409
8	.5902060	x	---	--	.1602931

Table 9. Frequencies of a Two-Substructure Clamped-Free Beam

Elastic Mode Number	$N_A = 5$, $N_B = 4$		$N_A = 5$, $N_B = 4$		Exact
	1st order (MacNeal)	% error	Hou	% error	
1	.0002086	0.05	.0002807	34.63	.0002085
2	.0015875	0.02	.0017529	10.44	.0015872
3	.0061381	0.14	.0072018	17.49	.0061297
4	.0170057	0.55	.0228352	35.02	.0169130
5	.0385203	0.69	.0415545	8.62	.0382562
6	.0783702	5.52	---	--	.0742702
7	.3928161	x	---	--	.1573651

Table 10. Frequencies of a Two-Substructure Free-Free Beam

Truss examples - MacNeal method versus Craig-Bampton method. - The Benfield truss of Fig. 3 was used in a study comparing the results obtainable by the first-order method with results obtained by use of the Craig-Bampton method. The results are shown in Table 11. The exact frequencies are the same as those given in Table 1, and were obtained using all of the original physical coordinates of the coupled system.

Since the Craig-Bampton method employs junction coordinates as well as substructure normal mode coordinates, the first-order method and Craig-Bampton method are compared on the basis of total number of system modes (N_{tot} = 16). Since no convergence studies were carried out, no strong conclusions can be reached about the comparison of MacNeal's method with the Craig-Bampton method, but Table 11 suggests that the MacNeal method produces results of accuracy comparable to those produced by the Craig-Bampton method. The Craig-Bampton method produces the best results for the low-frequency modes. The MacNeal method is not quite as accurate for these modes, but does better for the modes in the middle range of frequencies.

Elastic Mode Number	$N_A = N_B = 8$		$N_A = N_B = 5, N_j = 6$		Exact
	1st order (MacNeal)	% error	Craig-Bampton	% error	
1	0.004402	0.25	0.004391	0.00	0.004391
2	0.018377	0.26	0.018331	0.01	0.018329
3	0.030997	1.60	0.030527	0.06	0.030508
4	0.041740	0.36	0.041664	0.18	0.041589
5	0.069022	0.64	0.068734	0.22	0.068585
6	0.099727	0.97	0.098938	0.17	0.098770
7	0.116246	2.01	0.126051	10.61	0.113959
8	0.125738	2.76	0.144412	18.02	0.122362
9	0.151118	0.28	0.161327	7.05	0.150701
10	0.160644	3.54	0.247411	58.82	0.155147
11	0.231554	33.04	0.361008	x	0.174052
12	0.352010	75.15	0.506162	x	0.200979
13	1.524661	x	1.030503	x	0.215105

Table 11. Frequencies of Two-Substructure Benfield Truss by MacNeal Method and by Craig-Bampton Method

Grid examples - MacNeal method versus Craig-Bampton method for cantilever and free-free grid structures. - The grid structure shown in Fig. 5 was used for further comparison of the MacNeal method and the Craig-Bampton method. A similar free-free grid was also analyzed. In these studies a consistent mass matrix was employed.

Table 12 shows the results obtained for the first twenty modes of the cantilever grid. The column labelled "exact" is for the 72 d.o.f. original structure. For smaller numbers of total modes, the MacNeal method produces considerably better results than the Craig-Bampton method.

Figure 10 shows the number of modes accurate to within 0.5% as computed by each of the two methods. (The results shown in Fig. 10 include all the "0.5% modes" among the total number of modes calculated, i.e., 20, 24, 28, 32, even though only twenty modes are tabulated in Table 12.)

Table 13 shows the results obtained for the first twenty frequencies of a free-free grid structure as obtained by the MacNeal method and by the Craig-Bampton method. No exact values are available because of limitations on the size problem which could be handled by the eigensolver being used. It is noted that the frequencies are quite close, for the most part, with the maximum difference being only about 2.5%.

Elastic Mode Number	EXACT	$N_{tot} = 20$ $N_A = 11$, $N_B = 9$		$N_{tot} = 20$ $N_A = 5$, $N_B = 3$, $N_j = 12$	
		MacNeal	% error	Craig-Bampton	% error
1	.00006210	.00006210	0.00	.00006211	0.01
2	.00025109	.00025110	0.00	.00025115	0.02
3	.00163979	.00164073	0.05	.00164660	0.41
4	.00238797	.00238799	0.00	.00239788	0.41
5	.00394372	.00394463	0.02	.00395306	0.23
6	.00819127	.00820367	0.15	.00871273	6.36
7	.00862821	.00865644	0.32	.00881859	2.20
8	.01806006	.01808477	0.13	.01857390	2.84
9	.01991494	.01998109	0.33	.02188961	9.91
10	.02254916	.02260244	0.23	.02271096	0.71
11	.02744331	.02752603	0.30	.03864739	40.82
12	.03262871	.03298812	1.10	.06218932	90.59
13	.04493968	.05362282	19.32	.08120924	x
14	.05150864	.05581855	8.36	.12613476	x
15	.06175304	.06373244	3.20	.20728453	x
16	.06664190	.06884813	3.31	.36264343	x
17	.06963443	.17950904	x	.53033012	x
18	.08534049	.25447977	x	1.05181024	x
19	.08680764	.69330843	x	2.45246230	x
20	.08914933	1.32773903	x	5.23913299	x

Table 12. Frequencies of Cantilever Grid Structure

Elastic Mode Number	$N_{tot} = 24$ $N_A = 14$, $N_B = 10$		$N_{tot} = 24$ $N_A = 7$, $N_B = 5$, $N_j = 12$		$N_{tot} = 28$ $N_A = 16$, $N_B = 12$	
	MacNeal	% error	Craig-Bampton	% error	MacNeal	% error
1	.00006210	0.00	.00006210	0.00	.00006210	0.00
2	.00025110	0.00	.00025109	0.00	.00025109	0.00
3	.00164035	0.03	.00164019	0.02	.00164025	0.02
4	.00238799	0.00	.00239012	0.09	.00238797	0.00
5	.00394406	0.00	.00394433	0.01	.00394400	0.00
6	.00820253	0.13	.00819496	0.04	.00819978	0.10
7	.00863702	0.10	.00867873	0.58	.00863315	0.05
8	.01807972	0.10	.01825831	1.09	.01806091	0.00
9	.01996598	0.25	.01997539	0.30	.01993582	0.10
10	.02257782	0.12	.02267290	0.54	.02255448	0.02
11	.02750739	0.23	.02750874	0.23	.02750444	0.22
12	.03289693	0.82	.03320131	1.75	.03266930	0.12
13	.04507813	0.30	.05276010	17.40	.04505674	0.26
14	.05574645	8.22	.05686502	10.39	.05158030	0.13
15	.06250395	1.21	.06696988	8.44	.06177593	0.03
16	.06861338	2.95	.08138276	22.11	.06858598	2.91
17	.07109523	2.09	.27636744	x	.06969506	0.08
18	.08733079	2.33	.35125316	x	.08557656	0.27
19	.09138064	5.26	.39979778	x	.08701777	0.24
20	.10946900	22.79	.53601805	x	.09134459	2.46

Table 12 (cont.). Frequencies of Cantilever Grid Structure

Elastic Mode Number	$N_{tot} = 28$ $N_A = 10$, $N_B = 6$, $N_j = 12$		$N_{tot} = 32$ $N_A = 18$, $N_B = 14$		$N_{tot} = 32$ $N_A = 12$, $N_B = 8$, $N_j = 12$	
	Craig-Bampton	% error	MacNeal	% error	Craig-Bampton	% error
1	.00006210	0.00	.00006210	0.00	.00006210	0.00
2	.00025109	0.00	.00025109	0.00	.00025109	0.00
3	.00163996	0.01	.00163998	0.01	.00163989	0.00
4	.00238879	0.03	.00238797	0.00	.00238814	0.00
5	.00394429	0.01	.00394398	0.00	.00394381	0.00
6	.00819481	0.04	.00819423	0.03	.00819336	0.02
7	.00863617	0.09	.00863294	0.05	.00863058	0.02
8	.01822469	0.91	.01806079	0.00	.01806936	0.05
9	.01995132	0.18	.01993480	0.09	.01992609	0.05
10	.02267161	0.54	.02255635	0.02	.02255262	0.01
11	.02748344	0.14	.2746659	0.08	.02746586	0.08
12	.03313560	1.55	.03266878	0.12	.03265385	0.07
13	.04505185	0.24	.06505075	0.24	.04498599	0.10
14	.05672962	10.13	.05157360	0.12	.05157714	0.13
15	.06272967	1.58	.06177415	0.03	.06186679	0.18
16	.06695281	0.46	.06735587	1.07	.06694378	0.45
17	.07023630	0.86	.06967776	0.06	.06967930	0.06
18	.08792538	3.02	.08553947	0.23	.08547908	0.16
19	.08987727	3.53	.08699608	0.21	.08694733	0.16
20	.12568251	40.97	.09114901	2.24	.08962024	0.52

Table 12 (cont.). Frequencies of Cantilever Grid Structure

Elastic Mode Number	MacNeal $N_A = 20$, $N_B = 15$ $N_{tot} = 35$	Craig-Bampton $N_A = 12$, $N_B = 8$, $N_j = 15$ $N_{tot} = 35$
1	.00045914	.00045913
2	.00091210	.00091192
3	.00197905	.00197929
4	.00286973	.00286953
5	.00399206	.00399188
6	.00680185	.00679642
7	.01032129	.01032054
8	.01156372	.01156373
9	.01462129	.01472953
10	.01979609	.01986503
11	.02500327	.02500680
12	.02542485	.02538976
13	.03188867	.03237293
14	.03479776	.03476012
15	.05306692	.05435942
16	.05514919	.05609568
17	.05588742	.06071017
18	.06206941	.06240902
19	.06640768	.06484146
20	.08028079	.07861373

Table 13. Frequencies for Two-Substructure Free-Free Grid

Testing Requirements

The free-interface methods described in this report, in particular the first-order method, are compatible with dynamic test procedures, as was pointed out by Rubin (ref. 6). Although considerable work needs to be done in exploring the relationship of these methods to dynamic test procedures, several comments may be made on the basis of the equations presented in this report.

The first-order method requires the substructure information indicated in Eqs. (115) and (117):

(1) Λ_k - square of natural frequencies of substructure free-interface modes to be kept

(2) Φ_k - normalized (with respect to the mass matrix) free-interface mode shapes of modes to be kept

(3) $G^{(1)}_{jj}$ - residual flexibility at junction coordinates

Items (1) and (2) are standard items which are determined in mode survey tests. The only complicating factor is that the modes are to be normalized with respect to the mass matrix.

The determination of the residual flexibility at junction coordinates appears to be relatively straightforward for constrained substructures. However, since $G^{(1)}_{jj}$ is a submatrix of $G^{(1)}_{a}$, which is determined as the difference of two flexibility matrices, Eq. (114), the sensitivity of this matrix to measurement errors should be thoroughly explored.

For unconstrained substructures the determination of the residual flexibility matrix requires a constrained flexibility matrix, G_c, and a transformation matrix A, which, by Eq. (142), involves the mass matrix and rigid-body modes. Equations (149) defines the flexibility matrix modified to account for rigid-body modes. Considerable study is needed to determine: (a) whether Eq. (149) provides the best way to treat rigid-body modes, and (b) whether Eq. (149) is sensitive to measurement errors.

CONCLUSIONS AND RECOMMENDATIONS

The studies of fixed-interface methods indicate that:

(1) Reduction of the number of junction coordinates is feasible since this produces results of accuracy comparable to that obtained when substructure normal modes are reduced.

(2) Reduction of junction coordinates may be based on:
   (a) Ritz representation of junction coordinates using Ritz vectors provided by the analyst.
   (b) Guyan reduction of junction coordinates using a static reduction of coordinates, with the retained coordinates selected by the analyst.
   (c) Modal reduction of junction coordinates, using "junction modes" as Ritz vectors and using frequency ratio or modal participation factor to determine the coordinates to be retained.

(3) Although the choice of method for reducing the number of junction coordinates is dependent, to some extent , on the problem to be solved, modal reduction has two advantages not offered by the other two methods:
   (a) The calculation of modal participation factors is very simple.
   (b) The final equations are of a form that could lead to a very efficient eigensolution algorithm if advantage were taken of

the fact that the generalized stiffness matrix is diagonal. A disadvantage is that a preliminary eigensolution for junction modes is required.

(4) Error analysis, i.e., determination of the frequency "error" introduced by omission of a particular Ritz vector (mode), may be conducted for any of the three proposed methods. The calculations are somewhat tedious except for the modal reduction method.

(5) Before investing further effort in implementing any of the above-named methods for reduction of junction coordinates, an attempt should be made to create an efficient computer program for implementing the original Craig-Bampton equation, Eq. (23). It should be possible to create an efficient power iteration program, since K_{ii} is diagonal and K_{jj} will be narrowly banded or, at worst, banded with only a few submatrices outside of the band. If such a program were available, it would be a straightforward matter to provide an option for modal reduction of junction coordinates.

Free-interface substructure models suggested by MacNeal and Rubin have been studied. Equations for coupling substructures to form systems have been presented and a number of example problems involving two substructures have been solved. On the basis of these studies, it is concluded that:

(1) Only substructure normal mode coordinates are retained in the final system equations of motion, yet, both first-order (MacNeal) and second-order (Rubin) free-interface methods produce accuracies

comparable to those produced by Hurty-type fixed-interface methods.

(2) The second-order (Rubin) method requires additional calculations, and further study is required to establish whether the improvement in results is sufficient to justify the added computational effort.

(3) The first-order method appears to be compatible with dynamic test procedures, but further study is needed, particularly with respect to unconstrained substructures.

(4) "Rubin-type" methods appear to give upper bounds to the system frequencies and to be rapidly convergent. Further study of error bounds is required, however, to confirm these points.

(5) Mode shape and stress errors should be investigated for "Rubin-type" methods and should be compared with those produced by Hurty-type methods.

REFERENCES

1. Hurty, W.C.: Dynamic Analysis of Structural Systems Using Component Modes. AIAA Journal, vol. 3, no. 4, April 1965, pp. 678-685.

2. Craig, R.R. Jr.; and Bampton, M.C.C.: Coupling of Substructures for Dynamic Analysis. AIAA Journal, vol. 6, no. 7, July 1968, pp. pp. 1313-1319.

3. Benfield, W.A.; Bodley, C.S.; and Morosow, G.: Modal Synthesis Methods. NASA Symposium on Substructure Testing and Synthesis, Aug. 1972.

4. Benfield, W.A.; and Hruda, R.F.: Vibration Analysis of Structures by Component Mode Substitution. AIAA Journal, vol. 9, no. 7, July 1971, pp. 1255-1261.

5. Craig, R.R. Jr.; Chang, C-J.: Substructure Coupling with Reduction of Interface Coordinates - Fixed-Interface Methods. TICOM Rep. 75-1, Texas Institute for Computational Mech., The Univ. of Texas at Austin, Jan. 1975.

6. Rubin, S.: An Improved Component-Mode Representation. AIAA Paper 74-386, April 1974.

7. MacNeal, R.H.: A Hybrid Method of Component Mode Synthesis. Computers and Structures, vol. 1, 1971, pp. 581-601.

8. Klosterman, A.L.: On the Experimental Determination and Use of Modal Representations of Dynamic Characteristics. Ph.D. Thesis, Univ. of Cincinnati, 1971.

9. Hurty, W.C.: Introduction to Modal Synthesis Techniques. ASME Winter Meeting, Nov. 1971.

0. Kuhar, E.J.; and Stahle, C.V.: A Dynamic Transformation Method for Modal Synthesis. AIAA Journal, vol. 12, no. 5, May 1974, pp. 672-678.

1. Anderson, R.G.; Irons, B.M.; and Zienkiewicz, O.C.: Vibration and Stability of Plates Using Finite Elements. Int. J. Solids and Structures, vol. 4, 1968, pp. 1031-1055.

2. Timoshenko, S.P.; Young, D.H.; and Weaver, W. Jr.: Vibration Problems in Engineering. J. Wiley & Sons, 1974, pp. 479-481.

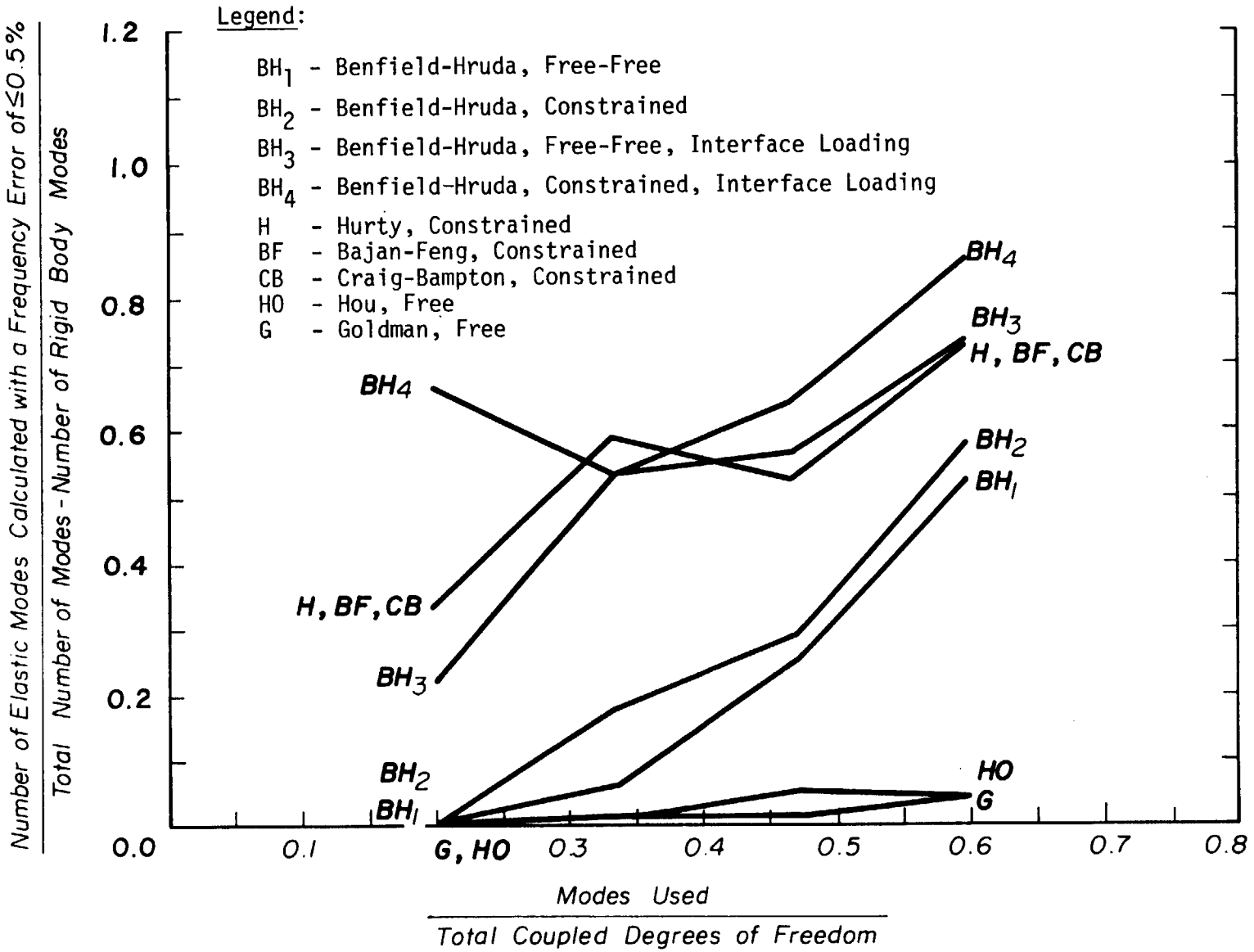

FIG. 1. COMPARISON OF METHODS WITH FREQUENCY ERROR OF ≤ 0.5%

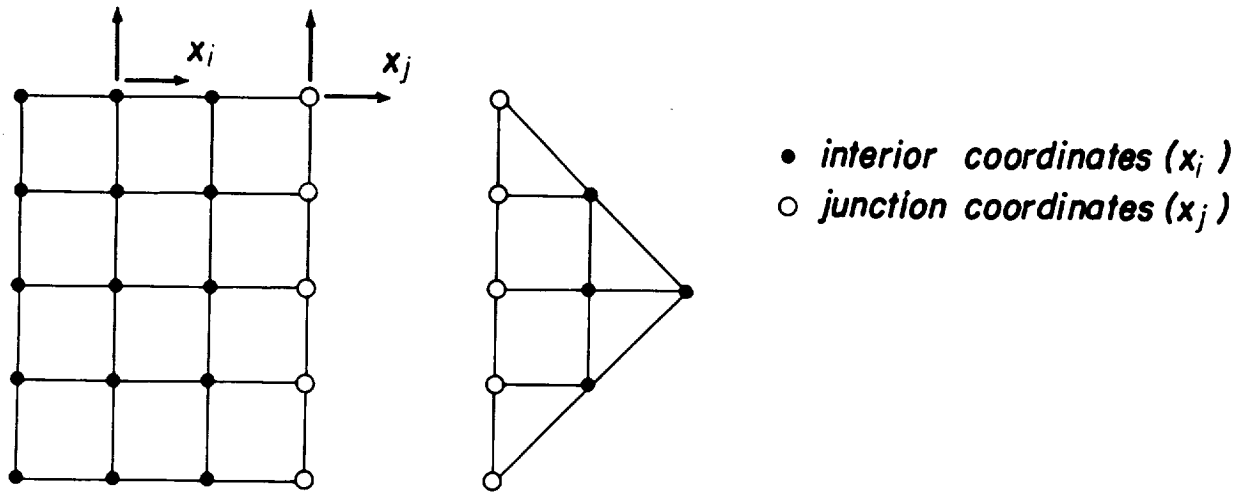

FIG. 2. SUBSTRUCTURE COORDINATES

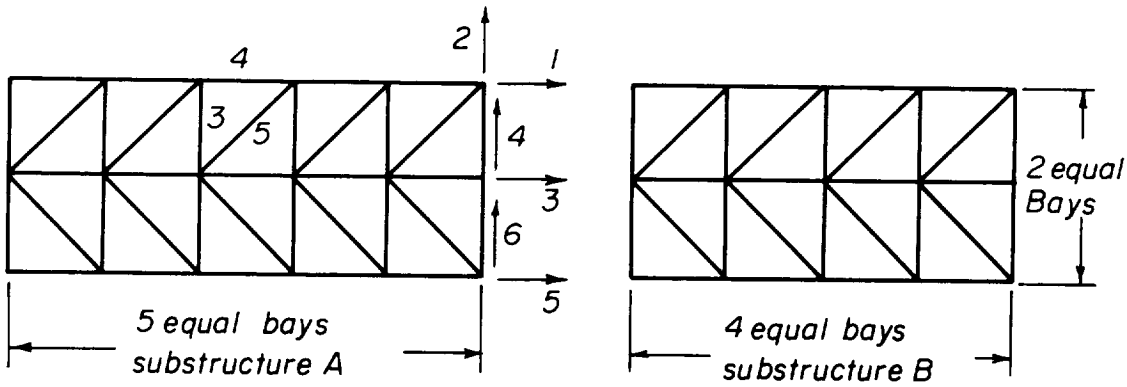

FIG. 3. TWO SUBSTRUCTURE BENFIELD TRUSS

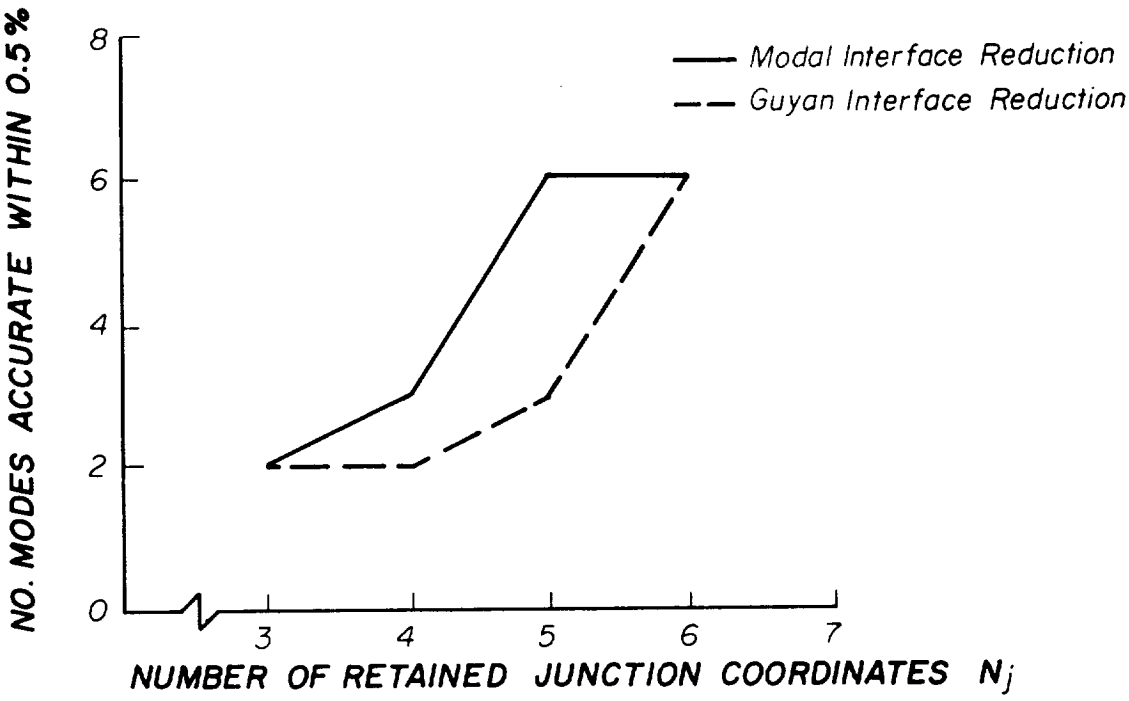

FIG. 4. MODAL INTERFACE REDUCTION vs GUYAN INTERFACE REDUCTION FOR BENFIELD TRUSS

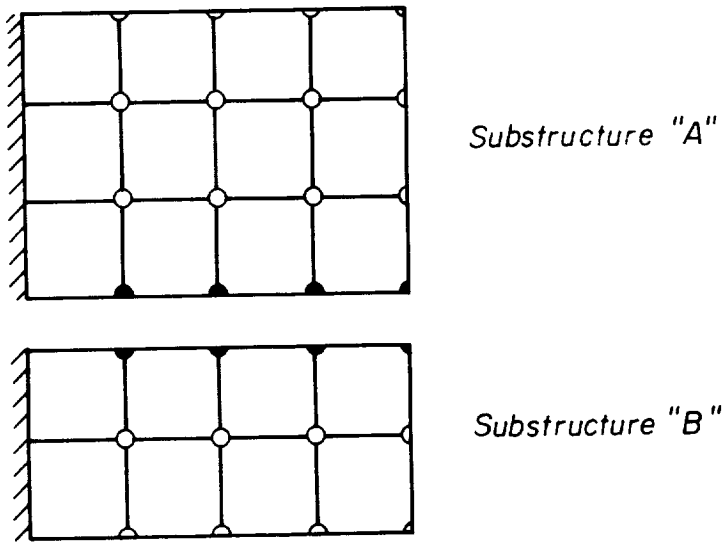

FIG. 5. CANTILEVER GRID STRUCTURE

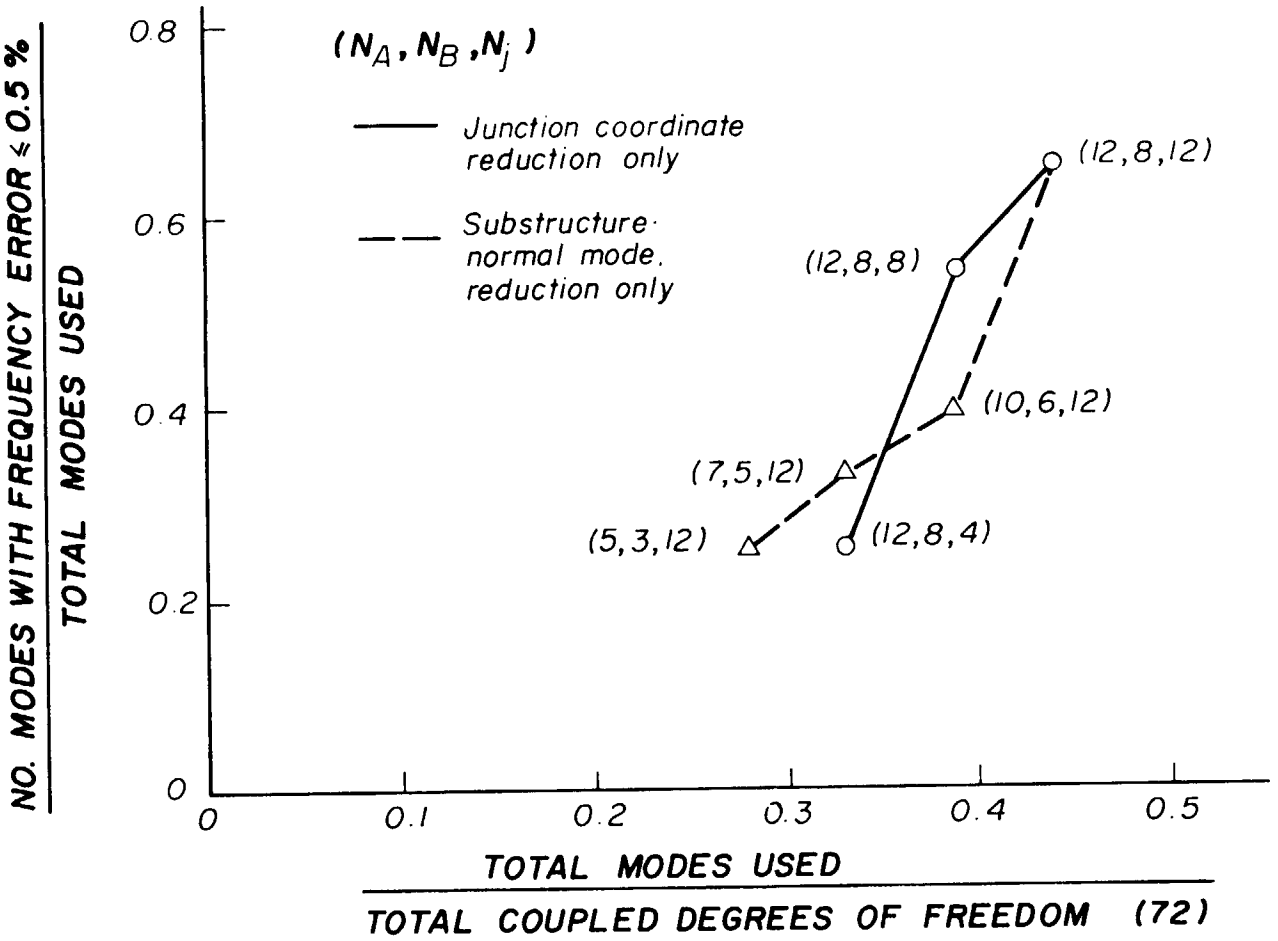

FIG. 6. NORMAL MODE REDUCTION vs JUNCTION MODE REDUCTION FOR CANTILEVER GRID STRUCTURE

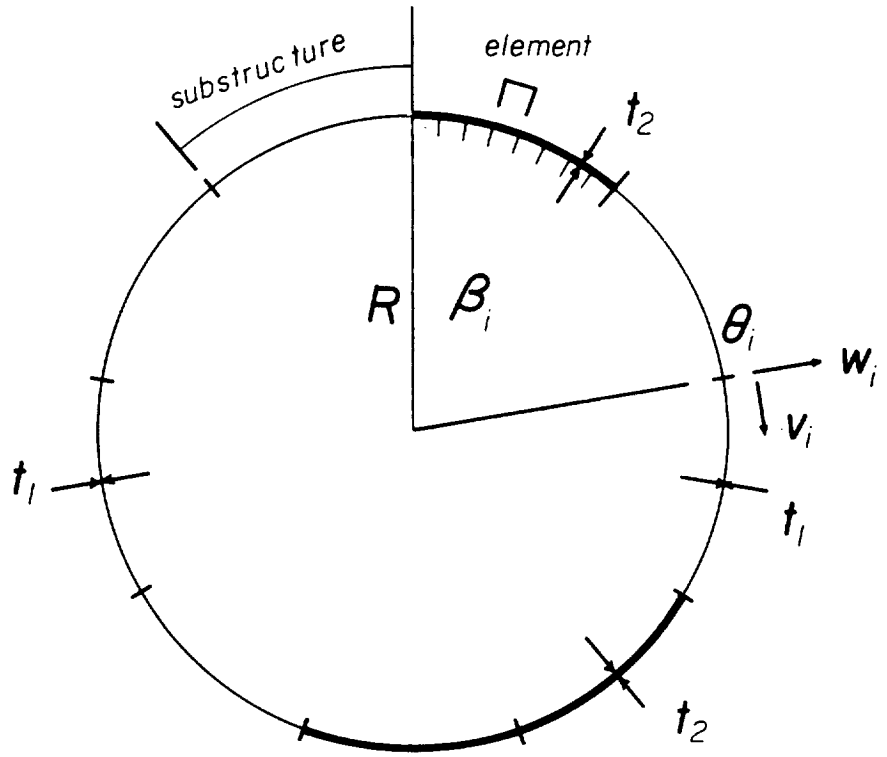

Case 1 $t_1 = t_2$ (uniform)

Case 2 $t_2 = 2t_1$

FIG. 7 . RING STRUCTURES

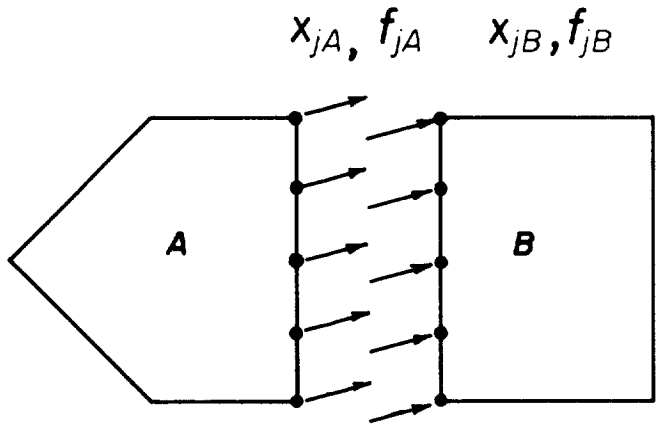

FIG. 8. TWO SUBSTRUCTURES WITH JUNCTION COORDINATES AND FORCES SHOWN SYMBOLICALLY

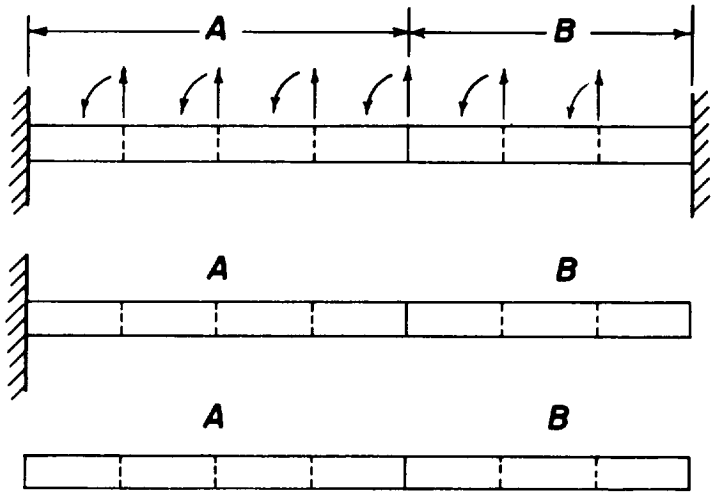

FIG. 9. BEAM CONFIGURATIONS

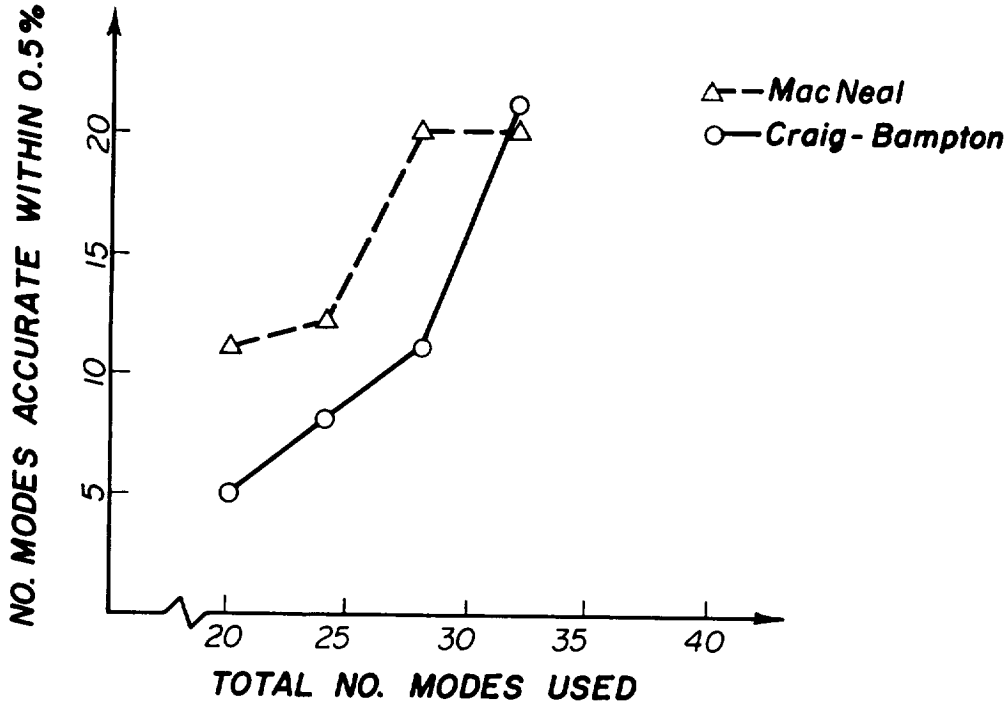

FIG. 10. COMPARISON OF MACNEAL AND CRAIG-BAMPTON METHODS FOR A CANTILEVER GRID STRUCTURE